



**UNIVERSIDAD AUTÓNOMA DE QUERÉTARO**  
**FACULTAD DE QUÍMICA**

**PROGRAMA DE POSGRADO EN ALIMENTOS DEL CENTRO DE LA  
REPÚBLICA (PROPAC)**

**DOCTORADO EN CIENCIAS DE LOS ALIMENTOS**

**Efecto del Superenfriamiento y la Viscosidad en la  
Formación de Redes Cristalinas en Sistemas Modelo a  
Base de Triacilglicéridos Puros y Aceites Vegetales.**

**Trabajo recepcional en su opción  
Artículos de Investigación**

**Que como parte de los requisitos para obtener el grado de**

**DOCTOR EN CIENCIAS DE LOS ALIMENTOS**

Presenta

**M. en C. ELENA DIBILDOX ALVARADO**

Director de Tesis

**DR. JORGE FERNANDO TORO VAZQUEZ**

**QUERÉTARO, QRO.**

**JUNIO, 2010**



Universidad Autónoma de Querétaro  
Facultad de Química  
Programa de Posgrado en Alimentos del Centro de la  
República (PROPAC)

**EFFECTO DEL SUPERENFRIAMIENTO Y LA VISCOSIDAD EN LA FORMACIÓN DE  
REDES CRISTALINAS EN SISTEMAS MODELO A BASE DE TRIACILGLICÉRIDOS  
PUROS Y ACEITES VEGETALES**

Opción de titulación:  
**Artículos de Investigación**

Que como parte de los requisitos para obtener el grado de  
**Doctor en Ciencias de los Alimentos**

Presenta:  
**M.C. Elena Dibildox Alvarado**

Dirigido por:  
**Dr. Jorge Fernando Toro Vazquez**

SINODALES

**Dr. Jorge Fernando Toro Vazquez**  
Presidente

**Dr. Alejandro G. Marangoni**  
Secretario

**Dr. Arturo Bello Pérez**  
Vocal

**Dr. Eleazar M. Escamilla Silva**  
Suplente

**Dr. Carlos Regalado González**  
Suplente

**Q.B. Magali E. Aguilar Ortiz**  
Director de la Facultad

  
Firma  
Firma  
Firma  
Firma  
Firma  
**Dr. Luis Gerardo Hernández Sandoval**  
Director de Investigación y  
Posgrado

**El presente trabajo fue realizado en:**

- **El Laboratorio de Fisicoquímica de Alimentos del Centro de Investigación y Estudios de Posgrado (CIEP) de la Facultad de Ciencias Químicas de la Universidad Autónoma de San Luis Potosí, bajo la dirección del Dr. Jorge Fernando Toro Vazquez, Profesor Investigador y Director de la Secretaría de Investigación y Posgrado de dicha Universidad.**
- **El Departamento de Ciencia de los Alimentos del Colegio de Agricultura de la Universidad de Guelph, en Guelph, Ontario Canadá, bajo la asesoría del Dr. Alejandro G. Marangoni, Profesor Investigador en Jefe de Canadá.**

## RESUMEN

Se estudió el comportamiento de mezclas de tripalmitina (TP) y triestearina (TS) 25:75 con trioleína (TO), aceites de cártamo alto en oleico (HOSfO) y de soya (SBO) previo a la nucleación de triacilgliceroles (TAGS) empleando espectroscopia de fluorescencia polarizada (FPS) y simulación mecánica molecular (MM). Adicionalmente, se determinó la energía libre de activación para la nucleación ( $\Delta G_c$ ) utilizando la ecuación de Fisher-Turnbull. Las temperaturas de cristalización empleadas (ej., 36°C-41°C en mezclas-TP y 46°C-51°C en mezclas-TS) se seleccionaron para obtener condiciones de superenfriamiento similares en ambas mezclas. Los resultados fueron estadísticamente analizados por ANOVA contrastando las medias de los tratamientos. La anisotropía de las mezclas de TP:HOSfO y TP:SBO aumentó a diferencia de la TP:TO y todas las mezclas -TS. Este comportamiento se asoció a un aumento en la microviscosidad de la fase líquida como consecuencia de la estructuración de los TAGS previo a su nucleación. Se realizó MM para entender las interacciones moleculares responsables de este comportamiento lo que indicó que las fuerzas de van der Waals son las responsables del aumento en la microviscosidad. Existe una interacción específica favorable particularmente cuando el aceite contiene TAGS con al menos un ácido palmítico, lo que induce en las mezclas una estructuración de los TAGS antes de la nucleación. En las mezclas-TS esto ocurrió antes de alcanzar las condiciones de superenfriamiento requeridas para la cristalización. Por consiguiente, la  $\Delta G_c$  en las mezclas TS:HOSfO y TS:SBO fue menor que la  $\Delta G_c$  de la TS:TO. En contraste, en las mezclas-TP, la estructuración de los TAGS ocurrió en función del tiempo bajo condiciones isotérmicas. Postulamos que las interacciones moleculares que ocurren en la fase líquida entre la TP y los TAGS con ácido palmítico resultan en el desarrollo de estructuras lamelares líquidas de TAGS mixtos, resultando en una mayor  $\Delta G_c$  a medida que la concentración de TAGS con ácido palmítico aumenta. Es necesario entender las interacciones moleculares entre TAGS en la fase líquida ya que están relacionadas con la cristalización qué, a su vez, determina las propiedades macroscópicas de productos lipídicos. Este trabajo versa en esta línea de investigación.

Palabras clave: Nucleación de triacilgliceroles, cristalización, espectroscopia de fluorescencia polarizada, mecánica molecular, energía libre de activación.

## SUMMARY

We have studied the pre-nucleation behavior of tripalmitin (TP) and tristearin (TS) blended in a 25:75 ratio with triolein (TO), high oleic safflower oil (HOSfO) and soybean oil (SBO) using fluorescence polarization spectroscopy (FPS), and molecular mechanics simulations (MM). We also determined the activation free energy to develop a stable nucleus ( $\Delta G_c$ ) using the Fisher-Turnbull equation. The crystallization temperatures used (i.e., 36°C-41°C in TP blends, and 46°C-51°C in TS blends) were selected to obtain similar supercooling conditions in both types of blends. The results were statistically analyzed using ANOVA and contrast among the treatment means. The FPS measurements showed that there is an increase in the anisotropy of TP:HOSfO and TP:SBO blends as opposed to TP:TO and all TS blends. This behavior is directly associated with an increase in the microviscosity of the liquid phase as a result of triacylglycerols (TAGS) structuring prior to the crystals' nucleation. We performed MM to understand the molecular interactions responsible for this behaviour. The results indicated that short range van der Waals interactions are responsible for the increase in microviscosity prior to TAGS crystallization. There seems to be a specific favourable interaction particularly when the oil contains TAGS with at least one palmitic acid in their composition, inducing a pre-nucleation structuring in the blends. In TS blends the molecular interaction occurred well before attaining supercooling conditions required for crystallization. As a result,  $\Delta G_c$  in TS:HOSfO and TS:SBO blends were lower than the  $\Delta G_c$  in the TS:TO blend. In contrast, in the TP blends TAGS structuring occurred as a function of time under isothermal conditions. We postulate that the molecular interactions occurring in the liquid phase between TP and TAGS with palmitic acid resulted in the development of mixed TAGS lamellar liquid structures. This resulted in higher  $\Delta G_c$  for TP nucleation as the concentration of TAGS containing palmitic acid increased in the blends. We need to understand the molecular interactions among TAGS in the liquid phase, since they relate to the TAGS crystallization process that in turn determines the macroscopic properties of lipid-based products. This study is included in this line of research.

Keywords: Triacylglycerols nucleation, crystallization, fluorescence polarization spectroscopy, molecular mechanics, activation free energy.

## **DEDICO ESTA TESIS**

*A DIOS, POR PERMITIRME VIVIR Y FLORECER EN SU CAMINO.*

*A **Roberto, Ale y Rolly**, por darme su cariño, paciencia y tiempo. Sin su apoyo hubiera sido imposible lograr esta meta. Para ustedes estoy, gracias por siempre.*

*A la memoria de mi Papá, Víctor, Paty, Carmela, Tere, Luis, Quino y Abuelo Fer.*

*A mi Mamá, por darme la vida y por todo.*

*A mis queridos hermanos, quienes de una u otra manera han sido un aliento para salir adelante: Martha, Fernando, Rosy, Maru, Dora, Estela, Yoly, Toño, Ma. Elena, Mague, Lucha, Anita y Gerardo (tu apoyo desencadenó mi mundo profesional, muchas gracias). A mi muy querida Tía Lichita, a mis entrañables Sobrinos y Cuñados.*

*A abuela Coco y a mí estimada familia González M. y respectivos.*

## AGRADECIMIENTOS

A mi director de tesis, **Dr. Jorge F. Toro Vazquez**, por su invaluable apoyo no solo en esta investigación sino en todo el desarrollo de mi vida profesional como maestro, como guía, como compañero de trabajo, pero sobretodo como amigo. Gracias Fernando.

A mi asesor de tesis, **Dr. Alejandro G. Marangoni**, por haber confiado en mí, por aceptarme en su grupo de investigación y darme su apoyo y amistad durante mi estancia en Canadá. Siempre le estaré agradecida.

A la Universidad Autónoma de Querétaro, en especial al Programa de Posgrado del Centro de la República de la Facultad de Química, por darme la oportunidad de estudiar en su programa y, a su Personal, por todo el apoyo dado.

Al Centro de Investigación y Estudios de Posgrado de la Facultad de Ciencias Químicas de la Universidad Autónoma de San Luis Potosí, por las facilidades brindadas durante la presente investigación y, a todo el personal de la Facultad, por su siempre incondicional ayuda.

Al Departamento de Ciencia de los Alimentos de la Universidad de Guelph, en Guelph, Ontario Canadá, por el apoyo brindado durante mi estancia.

Al PROMEP, por impulsar mi superación con su financiamiento mediante la beca 103.5/05/1624 y al CONACYT, por su apoyo a través del proyecto #25706. Mi reconocimiento para estos organismos.

A mis sinodales: Dr. Arturo Bello, Dr. Eleazar Escamilla y Dr. Carlos Regalado, por el tiempo dedicado en el seguimiento de esta investigación y por sus sugerencias. Igualmente, al Dr. Eduardo Castaño y Dr. Edmundo Mercado por su apoyo durante las reuniones de avance.

A mis amigas de andanzas y de toda la vida: Martha, Miriam, Rebe, Julieta, Paty, Marty, Paty C., Coco y Maru, por darle sabor a mis días.

A mis compañeros de trabajo: Juan Ángel, David, Conchita, Liz, Humberto, Mario y Latifeh, por su invaluable ayuda y convivencia diaria. A los tesisistas del Laboratorio, porque me han permitido crecer junto a ellos.

A mis muy queridos amigos de la Planta Piloto de I.A., gracias a todos por su ayuda y esos agradables e inolvidables momentos, muy en especial a Sandra y al Dr. Villalba. A todos mis compañeros y personal de I.A. y de la FCQ, por su afecto.

A todos a quienes han tenido que ver en mí andar, *GRACIAS*.

# ÍNDICE

	<b>Página</b>
Resumen	i
Summary	ii
Dedicatorias	iii
Agradecimientos	iv
Índice	v
I. INTRODUCCIÓN	1
II. RESUMEN EN EXTENSO Y PRIMER ARTÍCULO	6
III. RESUMEN EN EXTENSO Y SEGUNDO ARTÍCULO	12
IV. CONCLUSIONES GENERALES	18



# **I. INTRODUCCIÓN**

## **INTRODUCCIÓN**

Los aceites y grasas vegetales son sistemas multicomponentes que contienen distintas familias de triacilglicéridos (TAGS). En estos sistemas las relaciones moleculares que se producen entre las familias de TAGS determinan las condiciones termodinámicas (ej., superenfriamiento y supersaturación), que impulsan la formación de un sólido de la fase líquida, la organización de la fase sólida y su comportamiento de fase. La red tridimensional de cristales de TAGS resultante y su fase de comportamiento son factores importantes para determinar las propiedades físicas y funcionales (ej., reología, entrapamiento de la fase líquida, palatabilidad, apariencia y untabilidad) en productos tales como margarina, mantequilla y recubrimientos o rellenos para pasteles. Así, las complejas interacciones moleculares que se producen entre TAGS en la fase líquida bajo condiciones de superenfriamiento deben ser primero entendidas, ya que se relacionan directamente con el proceso de cristalización de TAGS que, en tiempo, determina las propiedades macroscópicas evaluadas por el consumidor en aceites vegetales y productos a base de grasa.

En principio todos los líquidos son isótropos: los movimientos moleculares dentro del líquido son brownianos por naturaleza y pueden ser descritos con la relación de Stokes–Einstein. Sin embargo, bajo ciertas circunstancias el fluido puede mostrar un movimiento preferencial o tener una restricción en su orientación. Es entonces dicho que el líquido está estructurado y por lo tanto muestra anisotropía. Ejemplos de estos líquidos estructurados son los cristales líquidos (LC). Su estado, ya sea proviniendo de la solución (liotrópico) o del fundido (termotrópico), es entre los límites de líquidos isótropos y cristales sólidos. A este estado también se le conoce como mesofase o bien estructura mesomórfica. Las propiedades ópticas anisotrópicas de los

cristales líquidos de fluidos poliméricos son como las de los sólidos regulares, pero sus moléculas presentan movimientos libres similares a las de los líquidos. Una de las particularidades de estas estructuras es que muestran una anisotropía espontánea y son fácilmente orientadas, siempre y cuando se encuentren como LC. Esta es una propiedad muy útil ya que un alto grado de alineación molecular en el estado líquido puede determinar las propiedades del producto final solidificado. Se ha sugerido que los TAGS también pueden mostrar anisotropía cuando se encuentran en estado de LC. El comportamiento de la fase de TAGS ha sido objeto de varios estudios debido a la importancia del polimorfismo en el procesamiento técnico de las grasas. Al respecto, diversos investigadores han propuesto las fases nemática, sméctica y discótica como disposiciones de arreglo molecular estructural para TAGS en fase líquida. Aunque no han establecido la organización estructural mesofásica de los TAGS y han utilizado como modelos sistemas simples, estas investigaciones apoyan el hecho de que las moléculas de TAGS de alguna manera están estructuradas en el estado líquido cristalino.

Debido a la aplicabilidad de los TAGS en mezclas multicomponentes en la industria alimentaria, cosmética y farmacéutica, la presente investigación es un intento para estudiar la estructura en estado líquido antes de la nucleación de sistemas más complejos. Los sistemas empleados fueron diseñados para proporcionar diferentes grados de compatibilidad molecular entre diferentes fases de disolventes (ej., trioleína, aceite de cártamo alto en trioleína y aceite de soya) con los TAGS saturados de interés (ej., tripalmitina y triestearina). Además, el tamaño y la forma de las estructuras de los LC cambian con la velocidad de difusión de las moléculas. Esto se traduce en un cambio en la viscosidad del sistema como función de la temperatura. Así, la viscosidad del aceite es una medida indirecta de la estructura o la

anisotropía de los TAGS en estado líquido, de manera que, cuando los aceites vegetales son enfriados, la viscosidad aumenta debido a una mayor organización de los TAGS. En estudios previos se ha demostrado que hay un aumento en la anisotropía (ej., medida por fluorescencia polarizada) en función del enfriamiento de los aceites, este aumento está relacionado al incremento en la viscosidad del medio. Por lo tanto, las medidas combinadas de viscosidad y anisotropía en aceites vegetales proporcionan información relacionada a la estructura líquida previa a la nucleación y su relación con la cristalización. Paralelamente al estudio de las interacciones moleculares que ocurren en los TAGS antes de su nucleación, investigamos su posible involucramiento en la energía libre de activación ( $\Delta G_c$ ) requerida para desarrollar un núcleo estable.

Por otro lado, las interacciones responsables del aumento en la anisotropía de un fluido son moleculares por naturaleza. El conocimiento de estas interacciones puede ser explorado por medio de simulaciones. En este trabajo, se realizó una simulación mecánica molecular (MM) para modelar el sistema con el fin de entender el papel de la energía involucrada en alcanzar un estado particular. MM es un método sencillo que describe la energía implicada en un sistema por medio de un conjunto de derivadas clásicas de funciones potenciales. En particular, a través de simulaciones, evaluamos aquí la estructura líquida de un sistema modelo binario de TAGS antes de la cristalización. Por lo tanto, creemos que el uso de simulaciones MM para estudiar mezclas complejas de TAGS (ej., grasas) cristalizados, proporcionaría información acerca de las interacciones energéticas responsables de la estructuración en estado líquido justo antes de que la nucleación se lleve a cabo.

## **II. RESUMEN EN EXTENSO Y PRIMER ARTÍCULO**

## **Estructuración Previa a la Nucleación de TAG Fundidos por Medio de Espectroscopia de Fluorescencia Polarizada y Simulación Mecánica Molecular**

E. Dibildox-Alvarado<sup>1</sup>, T. Laredo<sup>2</sup>, J. F. Toro-Vazquez<sup>3</sup>, A. G. Marangoni<sup>2</sup>

<sup>1</sup>Universidad Autónoma de Querétaro, DIPA-PROPAC, México. <sup>2</sup>University of Guelph, Department of Food Science, Guelph, Canadá <sup>3</sup>Universidad Autónoma de San Luis Potosí, Facultad de Ciencias Químicas, México.

### **RESUMEN**

En la presente investigación fue estudiado el comportamiento previo a la nucleación de la tripalmitina (TP) y la triestearina (TS) en mezclas 25:75 con trioleína (TO), aceite de cártamo alto en oleico (HOSfO) y aceite de soya (SBO), por medio de Espectroscopia de Fluorescencia Polarizada (FPS) y simulación Mecánica Molecular (MM). La composición de los aceites fue determinada por cromatografía líquida de alta resolución (HPLC) y reportada para los principales triacilglicéridos (TAGS), como la media ( $\pm$  desviación estándar) de al menos tres determinaciones independientes. Las temperaturas de cristalización empleadas (ej., 36°C a 41°C en mezclas de TP y 46°C a 51°C en mezclas de TS, con aumentos de grado en grado) fueron determinadas por calorimetría diferencial de barrido (DSC) y seleccionadas para obtener condiciones de supersaturación similares en ambas mezclas. Así mismo, de los termogramas correspondientes fueron obtenidas las propiedades térmicas de las mezclas. El estado polimórfico de las muestras cristalizadas fue obtenido por difracción de

rayos-X aplicando barridos de  $1^\circ/\text{min}$  desde  $1^\circ$  a  $40^\circ 2\theta$ . La viscosidad de las muestras durante la etapa de enfriamiento previa a la cristalización isotérmica fue obtenida cada  $5^\circ\text{C}$  con un espectrómetro mecánico equipado con sistema True-Gap, mientras que la anisotropía de las mezclas fue calculada usando las intensidades de fluorescencia de las mezclas previamente marcadas con 1,6-difenil-1,3,5-hexatrieno (DPH). Las intensidades fueron medidas en un espectrofotómetro de fluorescencia polarizada equipado con un monocromador de alta velocidad y cámara Peltier para control de temperatura. Los resultados fueron estadísticamente analizados por ANOVA contrastando las medias de los tratamientos. Por último, para obtener mayor información del grado de estructuración previo a la nucleación fueron realizadas simulaciones mecánicas moleculares empleando el software Chem3D. En todas las simulaciones fueron usadas 16 moléculas agrupadas en 4 filas de 4 moléculas, como se muestra en la figura 1.

Los termogramas con las propiedades térmicas de las mezclas mostraron dos endotermas, la primera a menor temperatura, asociada a la fusión de los TAGS de la TO, HOSfO y SBO, y la segunda a la mayor temperatura, correspondió a la fusión de la TP o TS según el sistema. La Tabla 1 resume las temperaturas de fusión de la segunda endoterma y sus correspondientes entalpías. Es claro que el TAG saturado en cada caso, funde a la misma temperatura para las tres mezclas correspondientes:  $58^\circ\text{C}$  y  $65^\circ\text{C}$  para las mezclas TP y TS respectivamente, siendo esto un indicador de que no hay interacciones específicas entre la TP o TS y los solventes utilizados.

Todos los patrones de difracción obtenidos mostraron picos aproximadamente a  $19^\circ$ ,  $23^\circ$  y  $24^\circ$  correspondiendo estos a los espacios de  $4.60$ ,  $3.85$  y  $3.70 \text{ \AA}$ , indicando que las mezclas cristalizaron como polimorfos  $\beta$  (ej., estructura triclínica). Como ejemplo, la figura 2

muestra difractogramas a temperaturas seleccionadas para mezclas de TP (Fig. 2a) y TS (Fig. 2b).

Las viscosidades obtenidas durante la fase de enfriamiento fueron graficadas en función de la anisotropía para cada una de las mezclas. La tabla 2 muestra los valores de la pendiente, la ordenada al origen y el coeficiente de correlación de las linealidades obtenidas. Los altos valores de  $R^2$  muestran que la viscosidad y la anisotropía varían linealmente, de aquí que la anisotropía, en el rango estudiado, es una medida de la viscosidad del volumen del sistema.

Aplicando la ecuación de Perrin modificada por Weber y col. para moléculas no esféricas, fueron calculadas las viscosidades de las mezclas para verificar la validez de esta aproximación. La tabla 3 muestra los valores de la viscosidad calculada y la determinada experimentalmente, ambas están en el mismo orden de magnitud, no obstante, la microviscosidad calculada es de manera consistente aproximadamente la mitad de la viscosidad experimental. La causa podría ser que, físicamente, la microviscosidad es un concepto diferente a la viscosidad del volumen de la mezcla, especialmente si el fluido está, de alguna manera, estructurado. Sin embargo, el resultado también podría implicar que la ecuación de Perrin no ajusta al sistema.

Los resultados de FPS a diferentes temperaturas mostraron que la anisotropía de las mezclas de TP:HOSFO y TP:SBO aumentó a diferencia de la TP:TO (Fig. 3). Este comportamiento fue directamente asociado a un aumento en la microviscosidad de la fase líquida como efecto de interacciones moleculares que conducen a la estructuración de la mezcla previa a la nucleación y crecimiento de los cristales. El efecto del solvente en las muestras de TP es diferente en cada caso. El que la mezcla de TP:TO no muestre incrementos implica que la estructuración del fluido no es debida a la presencia de trioleína en la mezcla. Según nuestra propuesta, esto debe ser un efecto debido a la presencia de



otros TAGS presentes en el HOSFO y el SBO. Además, los picos de anisotropía son mayores para las mezclas TP:SBO, indicando que el efecto de ordenamiento fue más fuerte en presencia de SBO como solvente en las mezclas. Para este efecto fue determinada la composición de TAGS en las mezclas (Tabla 4). En el caso de las mezclas TS, algunas temperaturas mostraron aumentos en la anisotropía pero los más consistentes fueron en mezclas con SBO. Podríamos hipotetizar que, de alguna manera, la presencia de uno o diferentes TAGS presentes en SBO inducen el efecto de ordenamiento en el fluido y, de estar presente, la concentración no fue lo suficientemente alta para lograr una estructuración en las mezclas TS:HOSFO.

Se realizó MM para entender las interacciones moleculares responsables del comportamiento de la anisotropía en las mezclas. El componente van der Waals (vdW) para un sistema de TP pura una vez minimizada la energía, fue de  $695 \pm 4$  kcal/mol. En contraste, la simulación de la TO pura resultó tener un valor de  $747 \pm 2$  kcal/mol. Esto indica que las fuerzas vdW son las responsables del comportamiento líquido o sólido de los TAGS y por lo tanto, causantes del aumento en la microviscosidad previo a su cristalización. La figura 4 muestra el promedio de los valores de la energía vdW para diversas mezclas de TP y sus análogos de TS. Las mezclas TP:PLL, TP:PLO y TP:POO tuvieron una energía vdW significativamente menor ( $P > 0.05$ ) que la mezcla TP:TO. En las mezclas de TS se encontró un comportamiento similar. Estos resultados indican también, que la presencia de moléculas que contienen al menos una cadena de ácido palmítico en su composición de TAGS, induce a un aumento en la microviscosidad de la mezclas previo a la nucleación. Por último, se estudió la aplicabilidad de estas conclusiones a TAGS de cadena larga. Nuestros resultados de MM mostraron que las mezclas hipotéticas de TS

y TAGS conteniendo ácido esteárico en su estructura, no tendrá una energía vdW lo suficientemente baja como para dar cuenta de un aumento en la microviscosidad.

En conclusión, este trabajo estudió el ordenamiento previo a la nucleación que ocurre en mezclas de TAGS saturados con diferentes aceites líquidos. Los experimentos de FPS nos dieron una visión sobre la estructuración a nivel microscópico que ocurre en esta etapa. Sin embargo, no estaba claro cuales interacciones eran las responsables de este efecto a nivel molecular. Se realizaron simulaciones de MM para abordar este aspecto. MM es una herramienta rápida y simple, pero poderosa, que puede proporcionar información complementaria a los datos experimentales. Obviamente, los resultados obtenidos necesitan ser cuidadosamente interpretados según las condiciones usadas en las simulaciones. Una vez que esto se logra, el resultado de aplicar este procedimiento es generalmente una mejor comprensión de las interacciones moleculares responsables de un determinado fenómeno observado experimentalmente. Utilizando MM hemos sido capaces de determinar que las interacciones de van der Waals son claves en la etapa anterior a la nucleación de grasas. También hemos demostrado que ocurre un comportamiento específico en función de la composición molecular de un TAG en particular. Estos resultados indican que las interacciones tanto generales como específicas desempeñan un papel importante en la etapa previa a la nucleación.

2 **Pre-Nucleation Structuring of TAG Melts Revealed**  
3 **by Fluorescence Polarization Spectroscopy and Molecular**  
4 **Mechanics Simulations**

5 **E. Dibildox-Alvarado · T. Laredo ·**  
6 **J. F. Toro-Vazquez · A. G. Marangoni**

7 Received: 17 February 2010/Revised: 8 April 2010/Accepted: 22 April 2010  
8 © AOCS 2010

9 **Abstract** We have studied the pre-nucleation behavior of  
10 tripalmitin (TP) and tristearin (TS) in blends with triolein  
11 (TO), high oleic safflower oil (HOSfO) and soybean oil  
12 (SBO) by means of fluorescence polarization spectroscopy  
13 (FPS) and molecular mechanics simulations (MM). The  
14 FPS measurements at different temperatures showed that  
15 there is an increase in the anisotropy of the TP:HOSfO and  
16 TP:SBO blends as opposed to the TP:TO sample. This  
17 increase is directly related to an increase in the microvis-  
18 cosity of the blend which is interpreted as a structuring step  
19 prior to the nucleation and growth of the crystals. A similar  
20 but less pronounced effect was also observed in the  
21 TS:SBO blends. We performed MM simulations in an  
22 attempt to understand the molecular interactions responsi-  
23 ble for this behavior. The simulation results have shown  
24 that short range van der Waals interactions are the ones  
25 responsible for the increase in the microviscosity of the  
26 blends prior to crystallization. Our results also indicate that  
27 the presence of molecules that contain at least one chain of  
28 palmitic acid in their triglyceride (TAG) composition will  
29 induce a pre-nucleation increase in the microviscosity of  
30 the blend in both TP and TS containing systems. Lastly, we  
31 studied the applicability of these conclusions to longer

chain TAG analogues. Our MM results show that hypo- 32  
theoretical blends of TS and TAGs containing stearic acid 33  
in their structure, will not have a low enough vdW energy to 34  
account for an increase in the microviscosity. Hence, there 35  
seems to be a specific interaction particularly favorable 36  
when the oil contains TAGs with at least one palmitic acid 37  
chain. 38

39  
40 **Keywords** Triglycerides · Structuring · Pre-nucleation ·  
41 Fluorescence polarization spectroscopy ·  
42 Molecular mechanics

43 **Introduction**

44 In principle all liquids are isotropic: the molecular motions 44  
within the fluid are Brownian in nature and can be 45  
described by the Stokes–Einstein relationship. However, 46  
under certain circumstances a fluid may display a prefer- 47  
ential motion or have an orientational restriction. It is then 48  
said that the fluid is structured and hence displays anisot- 49  
ropy [1]. Examples of these structured liquids are liquid 50  
crystalline (LC) polymers. The state of their solution 51  
(lyotropic) or melt (thermotropic) is between the bound- 52  
aries of solid crystals and isotropic liquids. This state is 53  
also referred to as a mesomorphic structure or a mesophase. 54  
The anisotropic optical properties of liquid crystal poly- 55  
meric fluids are like those of regular solids, but their 56  
molecules are free to move similar to liquids. One of the 57  
many interesting properties of these mesogenic structures 58  
is that they show spontaneous anisotropy and are easily 59  
oriented, provided that they are in a LC state. This is an 60  
extremely useful property because a high degree of 61  
molecular alignment in the fluid state can determine the 62  
properties of the solidified end product. This is essential, 63

A1 E. Dibildox-Alvarado · J. F. Toro-Vazquez  
A2 Facultad de Ciencias Químicas, Universidad Autonoma de San  
A3 Luis Potosi, San Luis Potosi, Mexico

A4 E. Dibildox-Alvarado  
A5 Universidad Autonoma de Queretaro, DIPA-PROPAC,  
A6 Querétaro, Mexico

A7 T. Laredo · A. G. Marangoni (✉)  
A8 Department of Food Science, University of Guelph,  
A9 Guelph, Canada  
A10 e-mail: amarango@uoguelph.ca

64 for example, for making high stiffness materials such as  
65 Kevlar (DuPont), Vectra (Hoechst Celanese) and Xydar  
66 (Amoco) among other classical examples.

67 It has been suggested that triacylglycerides (TAGs) also  
68 display anisotropy when in the LC state. The phase  
69 behavior of TAGs has been the subject of several studies  
70 due to the importance of polymorphism in technical fat  
71 processing.

72 Several groups have proposed different molecular  
73 arrangements for TAG melts. Namely, nematic and smectic  
74 phases have been the two mesophases most argued over on  
75 this subject. Cebula et al. [2] have proposed that TAGs in  
76 melts arrange themselves in a nematic phase characterized  
77 by molecular symmetry axes lined up parallel but without  
78 any positional order. Larsson, on the other hand, has postu-  
79 lated that the lipid molecules in the LC state arrange  
80 themselves in a lamellar-type of order typical of a smectic  
81 phase, where the molecules possess some positional order  
82 [3]. Sato and co-workers [4, 5] have shown through syn-  
83 chrotron radiation X-ray diffraction that TAGs in which  
84 one of the chains is unsaturated, display a LC phase  
85 characterized by lamellar ordering. However, their results  
86 are for pure TAGs that were quenched to temperatures well  
87 below the corresponding melting point and then heated  
88 rapidly to the target temperature. More recently, Corkery  
89 et al. [6] have proposed that molten TAGs form a discotic  
90 phase in which the triglyceride molecules exist in the liquid  
91 state with fully splayed chains, approximating "Y"-shapes.  
92 Regardless of the actual mesophase, all the work men-  
93 tioned above agrees on the fact that, TAG molecules are  
94 somehow structured in a LC-like state [2–9]. However,  
95 they all deal with model, single TAG component, samples.  
96 Due to the applicability of multicomponent TAG blends in  
97 food, cosmetic and pharmaceutical industries, the present  
98 work is an attempt to study the structure in the liquid state,  
99 prior to nucleation of these more complex systems. Our  
100 systems are meant to provide different degrees of molecu-  
101 lar compatibility between different solvent phases  
102 [triolein, safflower oil high in triolein, and soybean oil  
103 (SBO)] with the saturated TAGs of interest (tripalmitin and  
104 tristearin).

105 The shape and size of these LC structures changes with  
106 the diffusion rate of the molecules [8]. This translates into a  
107 change in the viscosity of the system as a function of  
108 temperature. Thus, oil viscosity is an indirect measurement  
109 of the structure or anisotropy of TAGs in the liquid state.  
110 When vegetable oils are cooled, the viscosity increases due  
111 to a higher organization of the TAGs [10]. Marangoni has  
112 shown that an increase in the anisotropy, as measured by  
113 fluorescence polarization, is observed upon cooling of oils,  
114 which is correlated to an increased viscosity of the medium  
115 [11]. Hence, the combined measurements of viscosity and  
116 anisotropy of vegetable oils provide information regarding

the liquid structure in a pre-nucleation state and its rela-  
117 tionship with crystallization. 118

119 Fluorescence polarization is a technique used to study  
120 the rotational movement of molecules in suspensions as  
121 well as in solutions [12] and provides information about  
122 concentration, binding events, and molecular structure,  
123 diffusion, mobility on membranes, and structure on sur-  
124 faces [13, 14]. In fluorescence polarization spectroscopy  
125 (FPS), a fluorophore is used as a probe to study the  
126 hydrodynamic behavior at the molecular level. Briefly, as  
127 the stiff fluorophore molecules in a fluid diffuse throughout  
128 the bulk, they undergo a precessional motion characterized  
129 by a rotational correlation time,  $\Phi$ . This is a time constant  
130 that characterizes the molecular rate of rotation. When  
131 polarized light impinges an ensemble of fluorophores, only  
132 those that are aligned with the plane of polarization will be  
133 excited. The emission can then undergo two different paths  
134 depending on the lifetime of the process: If the fluores-  
135 cence lifetime of the excited fluorescent probe is much  
136 longer than the rotational correlation time of the molecule  
137 it is bound to, the molecules will randomize in solution  
138 during the process of emission. As a result, the emitted  
139 light of the fluorescent probe will be depolarized. If, on the  
140 contrary, the fluorescence lifetime of the fluorophore is  
141 much shorter than the rotational correlation time, the  
142 excited molecules will stay aligned during the process of  
143 emission. In this case the emission will be polarized.  
144 Hence, the extent of depolarization is a measure the rota-  
145 tional correlation time. Because the molecules experience  
146 intermolecular friction forces that oppose their rotational  
147 diffusion, the extent of the depolarization is a measure of  
148 the anisotropy of the system and, in turn, of its microvis-  
149 cosity. A great deal of theoretical and empirical expres-  
150 sions have been derived for this purpose and the reader is  
151 referred to the works of Marangoni [11], Royer [15] and  
152 Mann and Krull [16] for a comprehensive review of the  
153 technique.

154 The interactions responsible for an increase in the  
155 anisotropy of a fluid are molecular in nature. The knowl-  
156 edge of these interactions can be explored by means of  
157 computer simulations. In this work, we have used molecu-  
158 lar mechanics (MM) to model the system in order to  
159 understand the role of energetics in achieving a particular  
160 state. MM is a simple method which describes the energy  
161 of the system in terms of a set of classically derived  
162 potential functions.

163 In particular, we evaluate here the liquid structure of  
164 binary model systems of TAGs prior to crystallization  
165 through MM simulations. Similar studies have been carried  
166 out in the past in different systems. For example, Nagarajan  
167 and Mayerson [17] have used MM to understand the role of  
168 energetics in the formation of the helical conformation of  
169 isotactic polypropylene in an attempt to understand

170 nucleation in the early stages of crystallization. Interest-  
 171 ingly, the work of Sato and co-workers [5] on monoun-  
 172 saturated TAGs notes that the ordering sequences between  
 173 the lamellar stacking and the lateral packing of these  
 174 molecules is very similar to that found upon crystallization  
 175 of isotactic polypropylene [18]. Hence, we believe that  
 176 using MM simulations to study complex TAG blends (e.g.  
 177 fats) crystallized under non-isothermal conditions, would  
 178 provide information regarding the energetic interactions  
 179 responsible for the structuring in the liquid state just before  
 180 nucleation takes place.

## 181 Materials and Methods

### 182 Triacylglycerides, Vegetable Oils, and Blend 183 Preparation

184 Tripalmitin (TP), tristearin (TS), and triolein (TO) with  
 185 purities higher than 99% were obtained from Sigma  
 186 Chemical Co. (St. Louis, MO). Refined, bleached and  
 187 deodorized high oleic safflower (HOSfO) and SBO were  
 188 obtained from local manufacturers. TAG composition of  
 189 the oils was determined by HPLC following the procedure  
 190 described by Perez-Martinez et al. [19] The composition of  
 191 major TAGS was reported as the mean ( $\pm$ standard devia-  
 192 tion) of at least three independent measurements. Each of  
 193 the saturated TP and TS were blended with either TO,  
 194 HOSfO, or SBO in a 25:75 (wt:wt) ratio. After 20 min at  
 195 80 °C with constant gentle stirring, the blends were stored  
 196 under nitrogen atmosphere at 2 °C in amber glass vials.

### 197 DSC Measurements

198 The crystallization and melting thermograms of the blends  
 199 were obtained by DSC using a TA Instruments Model  
 200 Q2000 (TA Instruments, New Castle, DE, USA). After  
 201 calibration of the equipment, blend samples (6–8 mg) were  
 202 sealed in aluminum pans, heated at 80 °C for 20 min and  
 203 then cooled to –60 °C at a rate of 10 °C/min. After 2 min  
 204 at this temperature the samples were heated to 80 °C at a  
 205 rate of 5 °C/min. In all cases an empty pan was used as  
 206 reference. The melting temperature ( $T_m$ ) and enthalpies  
 207 were calculated from the melting thermograms using the  
 208 equipment software.

### 209 X-Ray Diffraction

210 X-ray diffraction patterns of the crystallized blends  
 211 (14 mg) were obtained using a Rigaku Multiplex Powder  
 212 X-ray diffractometer (Rigaku, Japan) using a Cu source  
 213 X-ray tube ( $\lambda = 0.1542$  nm) at 40 kV and 44 mA. After  
 214 crystallizing the blend at the corresponding temperature

using a cooling rate of 10 °C/min, the X-ray diffraction  
 was recorded at scanning rate of 1° per min from 1° to 30°  
 $2\theta$ . The temperature was controlled with a Peltier system  
 and the results were analyzed using MDI's Jade 6.5 soft-  
 ware (Rigaku, Japan).

### Viscosity Measurements

The viscosity of the blends investigated was obtained at  
 different temperatures with a mechanical spectrometer  
 (Physica MCR 301, Anton Paar, Stuttgart, Germany)  
 equipped with TruGap system (P-PTD200/TG) using a  
 2.5-cm diameter parallel-plate geometry (PP25/TG). The  
 temperature was controlled by a Peltier system located in  
 both the base and top of the measurement geometry  
 through a Peltier-controlled hood (H-PTD 200). The con-  
 trol of the equipment was made through the software Start  
 Rheoplus/32 version 2.65 (Anton Paar, Graz-Austria).  
 After 20 min at 80 °C the system was cooled at a rate of  
 10 °C/min. At each 5 °C interval during the cooling stage,  
 the shear stress was determined by applying a logarithmic  
 shear rate sweep from 1 to 100 per s. Before the mea-  
 surements the system was allowed to achieve temperature  
 equilibrium for 5 min. The viscosity ( $\eta$ ) was determined as  
 the slope of shear stress versus shear rate by linear  
 regression. Two independent determinations were obtained  
 for each temperature.

### Anisotropy Measurements, During the Cooling Stage, Under Isothermal Crystallization Conditions

The anisotropy ( $r_s$ ) of the blends was calculated using the  
 fluorescence intensities of blends previously labeled with  
 a 1 mM of 1,6-diphenyl-1,3,5-hexatriene (DPH, Sigma,  
 St. Louis, MO, USA) solution in tetrahydrofuran (2  $\mu$ l/ml).  
 The intensities were measured with a polarizer spectro-  
 photometer (MD-5020 of Photon Technology International,  
 London, Ontario, Canada) equipped with a high speed  
 random access monochromator DeltaRAM using the  
 FeliX32 software. The prefixed wavelength was 360 nm  
 for excitation and 465 nm for emission. The fluorescence  
 intensities of the blends (250  $\mu$ l samples) were obtained  
 during the cooling (i.e. as a function of temperature) and  
 the isothermal stages (i.e. as a function of time) with the  
 observation polarizer parallel or perpendicular to the inci-  
 dent plane-polarized light. The two intensities were  
 obtained in independent experiments under the same time-  
 temperature conditions. In each case two independent  
 determinations were carried out. For the TP blends, the  
 anisotropy was measured every degree from 36 to 41 °C,  
 and for the TS blends every degree from 46 to 51 °C.  
 Although the range of temperatures is different for the TP  
 and TS blends, the supersaturation conditions are very

264 similar. The supersaturation ( $\ln\beta$ ) of the melts was calcu-  
265 lated as

$$\ln \beta = \frac{\Delta H}{RTT_m} \Delta T \quad (1)$$

267 where  $R$  is the gas constant,  $T$  the isothermal crystallization  
268 temperature.  $\Delta H$  the enthalpy of fusion,  $T_m$  the melting  
269 temperature for either TP or TS, and  $\Delta T$  is the difference  
270 between the melting temperature and the temperature of the  
271 experimental run [20]. For the anisotropy experiments,  $\ln\beta$   
272 ranges from 0.16 to 0.25 and from 0.15 to 0.24 for the TP  
273 and TS blends respectively. These ranges indicate that all  
274 samples had similar supersaturation conditions.

275 Temperature control was achieved with a Peltier sys-  
276 tem attached to a four position cuvette holder (Turret 400,  
277 Quantum Northwest). The anisotropy value ( $r_s$ ) was cal-  
278 culated under the cooling and isothermal stages of the  
279 blend crystallization considering the  $G$  correction for light  
280 scattering as described by Lakowicz [21]. The  $G$  correc-  
281 tion factors for the TP blends were 1.06, 1.02, and 0.97  
282 for TO, HOSfO, and SBO, respectively; and 1.09, 1.03  
283 and 0.96 for the TS blends with TO, HOSfO, and SBO,  
284 respectively.

## 285 Construction of the MM Initial Configuration

286 The general considerations to develop these TAGs lamellar  
287 structures used the following criteria:

- 288 • Saturated TAGs molecules had to be stackable in a  
289 chair-like conformation with parallel hydrocarbon  
290 chains at positions  $sn-1$  and  $sn-3$  and anti-parallel at  
291  $sn-2$  with a thickness of  $2L$ . Due to the unsaturation  
292 present in oleic acid this was more complicated in the  
293 case of triolein (TO) than for the fully saturated TP, and  
294 even more so for TAGs having different acyl chains  
295 such as PLL or PLO.
- 296 • For unsaturated TAGs two possible conformations were  
297 explored, such that the hydrocarbon chains at positions  
298  $sn-1$  and  $sn-3$  were pointing (a) in the same direction as  
299 the  $sn-2$  chain, and (b) away from the hydrocarbon  
300 chain at  $sn-2$  position.
- 301 • All unsaturations were in *cis* conformation
- 302 • Changes in the average tilt angle of the TAGs packing  
303 for the three major polymorphs,  $\alpha$ ,  $\beta'$  and  $\beta$ , had no  
304 effect on the energy minimization procedure.

305 Once these requirements were fulfilled, the actual initial  
306 configuration was found such that changes in dihedral  
307 angles of each TAG in a stack of four molecules led to a  
308 very similar minimization energy. This was taken as an  
309 indication of a minimum energy configuration. It should be  
310 noted that the vdW energy falls off as  $r^{-6}$ , but it can be cut  
311 off at much shorter distances. In this work, a cutoff value of

10 Å was used throughout, which increased the speed of  
the computation significantly.

All the simulations were performed with CS Chem3D  
Pro (CambridgeSoft v. 3.5.1), 16 molecules were used,  
stacked in 4 rows of 4 molecules, as shown in Fig. 1. The  
packing was such that the van der Waals radii of the atoms  
of adjacent molecules were just in contact with each other.  
The rows were arranged in both alternating and “sand-  
wiched” conformation. In the latter, two rows of the same  
molecule were in between two rows of the other molecule.  
The final result of the energy minimization for these two  
types of conformation was statistically determined to be  
equivalent. Hence we used these to calculate an average of  
4–6 sets for different mixes of TAGs.

Mixtures of more than two types of TAG proved to be  
extremely difficult to simulate as the number of variables in  
the initial configuration increased the uncertainty of the  
minimization procedure.

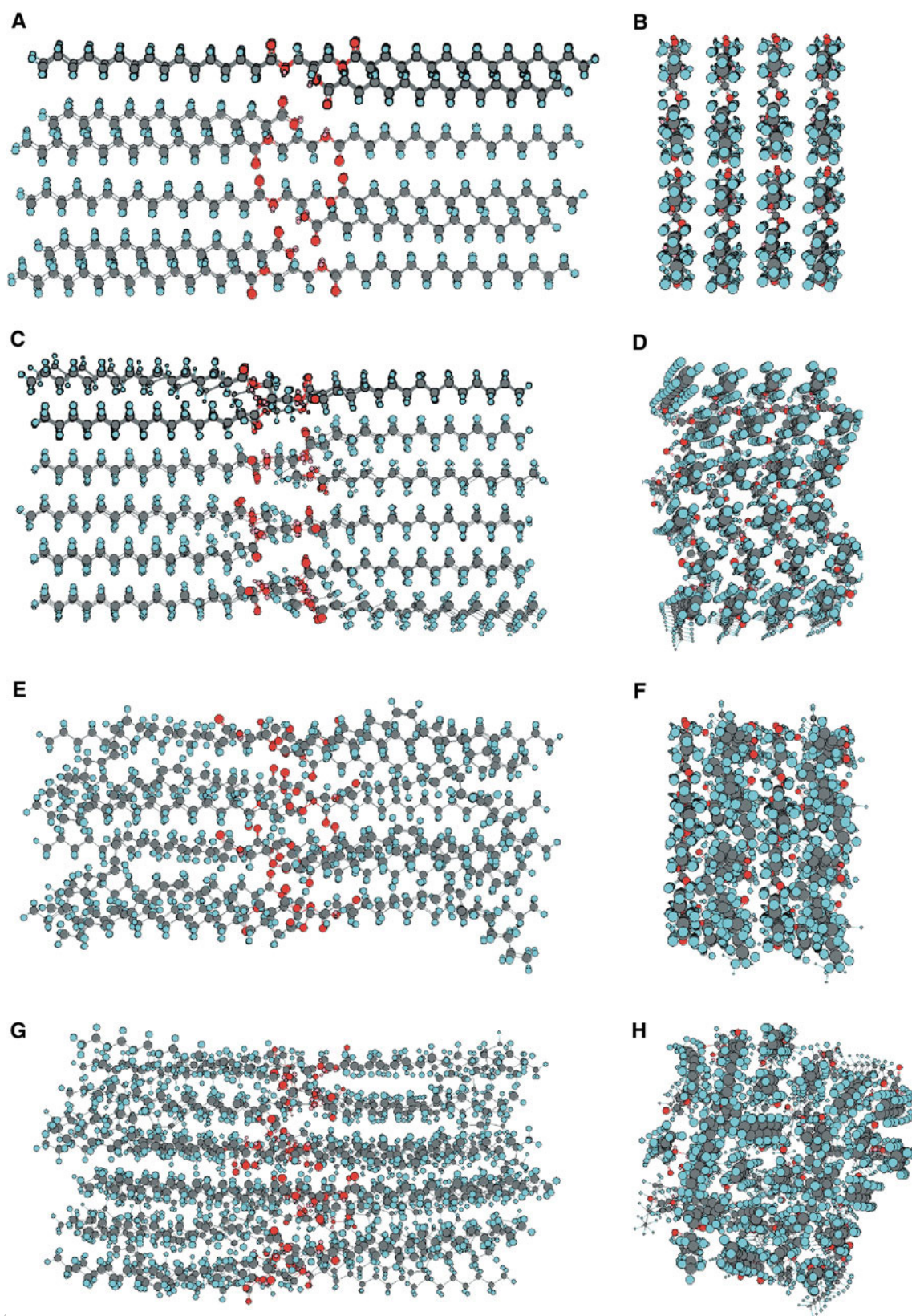
Once the initial configuration was set, the MM2 (an all  
atom force field based on the MM1 functional form [22])  
energy minimization was allowed to run until a root mean  
squared (RMS) gradient value of 0.014 was attained using  
a steepest descent minimization algorithm. If the slope of  
the potential energy surface becomes small enough, then  
the minimization has probably reached a local minimum on  
the potential energy surface, and the minimization termi-  
nates. Our convergence criterion was a good compromise  
between accuracy and speed of the simulation.

## Results

### Differential Scanning Calorimetry and X-ray Analysis

DSC measurements were performed on all blends. The  
melting thermograms (data not shown) consistently showed  
two endotherms. The lower temperature endotherm is  
associated with the melting of the TAGs from TO, HOSfO  
and SBO. The higher temperature endotherm corresponds  
to the melting of either TP or TS depending on the system.  
Table 1 summarizes the temperature values for the second  
endotherm and the corresponding enthalpies of melting as  
determined from the integration of the peak. It is clear that  
the fully saturated TAG in each case melts at about the  
same temperature for the three corresponding blends: about  
58 and 65 °C for the TP and TS blends respectively. This is  
an indication that there are no specific chain–chain inter-  
actions between the TP, or TS, and the solvents used in  
each mixture affecting the solubility and phase behavior of  
the blends.

The crystallinity of the blends was assessed by X-ray  
diffraction. Figure 2 shows the X-ray spectra for selected  
temperatures for both the TP blends (Fig. 2a) and the TS

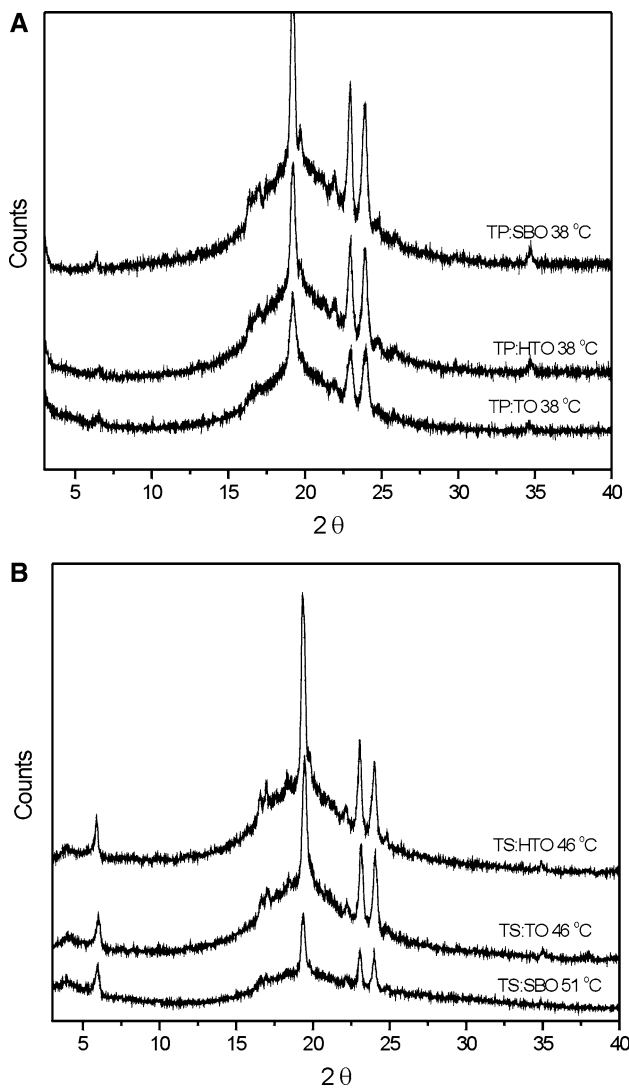


**Fig. 1** Stack of 16 molecules arranged in 4 rows of 4 molecules each. **a–d** For a TP stack. **e–h** For a TP:PLO mix in a 1:1 molecular ratio. The initial configurations are seen from a side (**a**, **e**) and front

(**b**, **f**) perspectives. After the energy minimization side (**c**, **g**) and front (**d**, **h**) views are shown for comparison

**Table 1** Melting temperatures and enthalpies of fusion for the TP and TS in their respective blends as determined from DSC heating measurements

Blend	$T_m$ (°C)	$\Delta H$ (kJ/mol)
TP:TO	$57.6 \pm 0.4$	$10.4 \pm 0.3$
TP:HOSfO	$57.5 \pm 0.4$	$10.58 \pm 0.2$
TP:SBO	$57.60 \pm 0.01$	$11.39 \pm 0.01$
TS:TO	$65.17 \pm 0.09$	$11.89 \pm 0.01$
TS:HOSfO	$64.7 \pm 0.5$	$12.8 \pm 0.1$
TS:SBO	$65.0 \pm 0.1$	$12.93 \pm 0.01$

**Fig. 2** X-Ray diffraction patterns. All TP blends (a) were crystallized at 38 °C. TS blends (b) crystallized at 46 or 51 °C as shown in the figure

blends (Fig. 2b). It is clear from the peaks at approximately 19°, 23° and 24° corresponding to spacings of 4.60, 3.85 and 3.70 Å, that the blends crystallized as the  $\beta$  polymorph (triclinic subcell structure).

## Fluorescence Polarization Spectroscopy

We have plotted the viscosity of the system determined from rheological measurements as a function of the anisotropy for each of the blends. Table 2 shows the values of slope, intercept and correlation of the linearity for these plots. The high  $R^2$  values clearly indicate that the viscosity and the anisotropy vary linearly, hence showing that the anisotropy, within the range studied, is a measure of the bulk viscosity of the system.

The Perrin equation has been modified by Weber et al. [23] to account for molecules that are not spherical (as is the case for most fluorescent tags), such that:

$$\frac{r_0}{r_s} = 1 + \frac{kT\tau}{\bar{\eta}v_0} \quad (2)$$

where  $r_s$  is the molecular anisotropy with  $r_o/r_s$  defined as the degree of depolarization,  $T$  the absolute temperature,  $\tau$  the average lifetime of the excited state,  $k$  the Boltzmann constant,  $\bar{\eta}$  is the microviscosity of the medium, and  $v_0$  the effective volume of the fluorescent probe. The maximum anisotropy value  $r_o$  is close to 0.4 for DPH [24]. The van der Waals volume of the DPH probe has been reported to be  $233 \text{ \AA}^3$  [24]. We have used Eq. 2 to determine the viscosity of the blends and verify the validity of this approach.

Table 3 shows the values of viscosity calculated using the Perrin equation and those determined experimentally for all blends at 55 °C. The fluorescence lifetime,  $\tau$ , of

**Table 2** Slope, intercept and correlation coefficient for plots of viscosity versus anisotropy for the TP (45–80 °C) and TS (55–80 °C) blends

Blend	Slope	y-Intercept ( $\times 10^{-3}$ )	$R^2$
TP:TO	0.762	9.4	0.996
TP:HOSfO	0.807	8.3	0.982
TP:SBO	0.674	9.9	0.984
TS:TO	0.719	9.9	0.983
TS:HOSfO	0.852	10.3	0.938
TS:SBO	0.852	9.6	0.972

**Table 3** Comparison between the bulk and calculated viscosities using Eq. 2 at 55 °C

Blend	Bulk viscosity $\eta$ (Pa s)	Microviscosity $\bar{\eta}$ (Pa s)
TP:TO	0.0297	0.0129
TP:HOSfO	0.0301	0.0130
TP:SBO	0.0278	0.0129
TS:TO	0.0310	0.0139
TS:HOSfO	0.0303	0.0119
TS:SBO	0.0294	0.0110



391 DPH is both temperature and solvent dependent. At 55 °C  
 392  $\tau$  is approximately 10 ns in heavy white paraffin oil [11].  
 393 The calculated and experimental viscosities are in the same  
 394 order of magnitude. However, there is a significant dis-  
 395 crepancy between the two. The calculated microviscosity is  
 396 consistently lower than the experimental values by  
 397 approximately a factor of 2. The reason could be a physical  
 398 one, in the sense that the microviscosity could be different  
 399 than the bulk viscosity of a blend, especially if the fluid is  
 400 somehow structured. However, this result could also imply  
 401 that the Perrin equation used here does not really hold for  
 402 our systems, due to some specific behavior of the blends.  
 403 Regardless, it is interesting that both sets of values are in  
 404 the same order of magnitude.

#### 405 Anisotropy as a Function of Time

406 Measurements of the normalized anisotropy,  $r_s/r_{t=0}$ , at  
 407 different supersaturation conditions are shown in Fig. 3a, b  
 408 and c for the TP:TO, TP:HOSfO and TP:SBO blends,  
 409 respectively and in Fig. 3d, e, and g for the TS analogues.  
 410 All the plots display an initial period of time where the  
 411 anisotropy is constant. Also, a decrease in the anisotropy at  
 412 the end of the experiment is common to all measurements  
 413 due to the scattering of light from newly formed nuclei. In  
 414 some cases, the anisotropy increases during the course of  
 415 the experiment before dropping at the end. Within these  
 416 features, the behavior of the TP and TS blends is different.  
 417 The time scale of the experiments for the TS samples is on  
 418 average three times longer (about 20 min) than for the TP  
 419 blends (between 5 and 7 min). This is an indication of a  
 420 higher  $\Delta G$  of nucleation for the TS blends, relative to the  
 421 TP blends.

422 The effect of the solvent in TP samples is different in  
 423 each case. TP:TO blends do not display an increase in the  
 424 anisotropy at any of the temperatures studied. For the  
 425 TP:HOSfO and TP:SBO samples, the measurements done  
 426 at 37, 38 and 40 °C in the former blends and those at all  
 427 temperatures for the latter one, display a clear increase in  
 428 the anisotropy. This increase in the anisotropy is related to  
 429 an increase in the microviscosity of the system and hence is  
 430 an indication of molecular interactions leading to the  
 431 structuring of the blend in a pre-nucleation state. The fact  
 432 that the TP:TO mixes show no increase, clearly implies  
 433 that the structuring of the fluid is not due to the presence of  
 434 triolein in the blend. We propose that it must be an effect  
 435 due to the presence of other TAGs present in the HOSfO  
 436 and SBO. Furthermore, the peak in anisotropy is highest  
 437 for the TP:SBO blends, indicating that the strongest  
 438 ordering effect is in the presence of SBO as the blend  
 439 solvent.

440 Several smaller features can be appreciated in Fig. 3. In  
 441 the measurements of TP:HOSfO at 36 and 38 °C and in

those at 46 and 47 °C for the TS:HOSfO mixes, after the  
 initial decrease in anisotropy due to the appearance of  
 crystals, the fluorescence polarization signal becomes very  
 weak and unstable and sometime spiking behavior is  
 observed due to artifactual scattering effects. The TAG  
 composition of HOSfO and SBO was determined in our  
 laboratory and it is summarized in Table 4. TAGs present  
 in a concentration of less than 5% in at least one of the  
 oils have been omitted from the table for simplicity.  
 Based on our FPS results, the interactions that lead to an  
 increase in the anisotropy are probably related to the  
 presence of TAGs other than TO (OOO in the table) in  
 the blends.

In the case of the TS blends, the general trend is slightly  
 different to that seen in the TP samples. Firstly, the TS:TO  
 samples at 49 and 50 °C show an increase in the anisotropy  
 that it is not seen for any of the TP:TO blends. Secondly,  
 the only increase in anisotropy seen in the TS:HOSfO  
 blends is a spike-like behavior seen at 47 °C. However, the  
 TS:SBO blends display a similar anisotropy increase to the  
 one observed in the TP:SBO mixes if only for the higher  
 temperature experiments. We believe that the increases  
 seen in the TS:TO and TS:HOSfO blends are due to arti-  
 facts and hence, are not representative of the behavior of  
 the blend, especially since they occur in the middle of the  
 temperature range. As a consequence, the only blends that  
 display some pre-nucleation ordering for the TS fat are  
 those dissolved in SBO. This is again an indication that  
 there is a TAG-specific interaction at the molecular level  
 responsible for the structuring of the blend prior to crys-  
 tallization. We could hypothesize that somehow the pres-  
 ence of one or several TAGs present in SBO induces this  
 ordering effect of the fluid and that, if at all present, the  
 concentration is not sufficiently high in the TS:HOSfO  
 blends to allow for the structuring effect. However our  
 results so far, do not allow for a better insight on the forces  
 and conditions necessary for this pre-nucleation increase in  
 the anisotropy to occur. We have used MM simulations to  
 address this aspect.

#### Molecular Mechanics Simulations

We have performed MM simulations in an attempt to  
 understand the molecular interactions responsible for the  
 experimental behavior seen in the anisotropy measure-  
 ments of the blends. The energies given by the Chem3D  
 program are divided into bonded and non-bonded interac-  
 tion energies. The latter one is further divided into Dipole/  
 dipole, long and short range van der Waals interactions. Of  
 these terms, only the short range van der Waals component  
 showed a consistent trend in the results within the repro-  
 ducibility of the method. The total energy and all other  
 components given as a result of the minimization showed

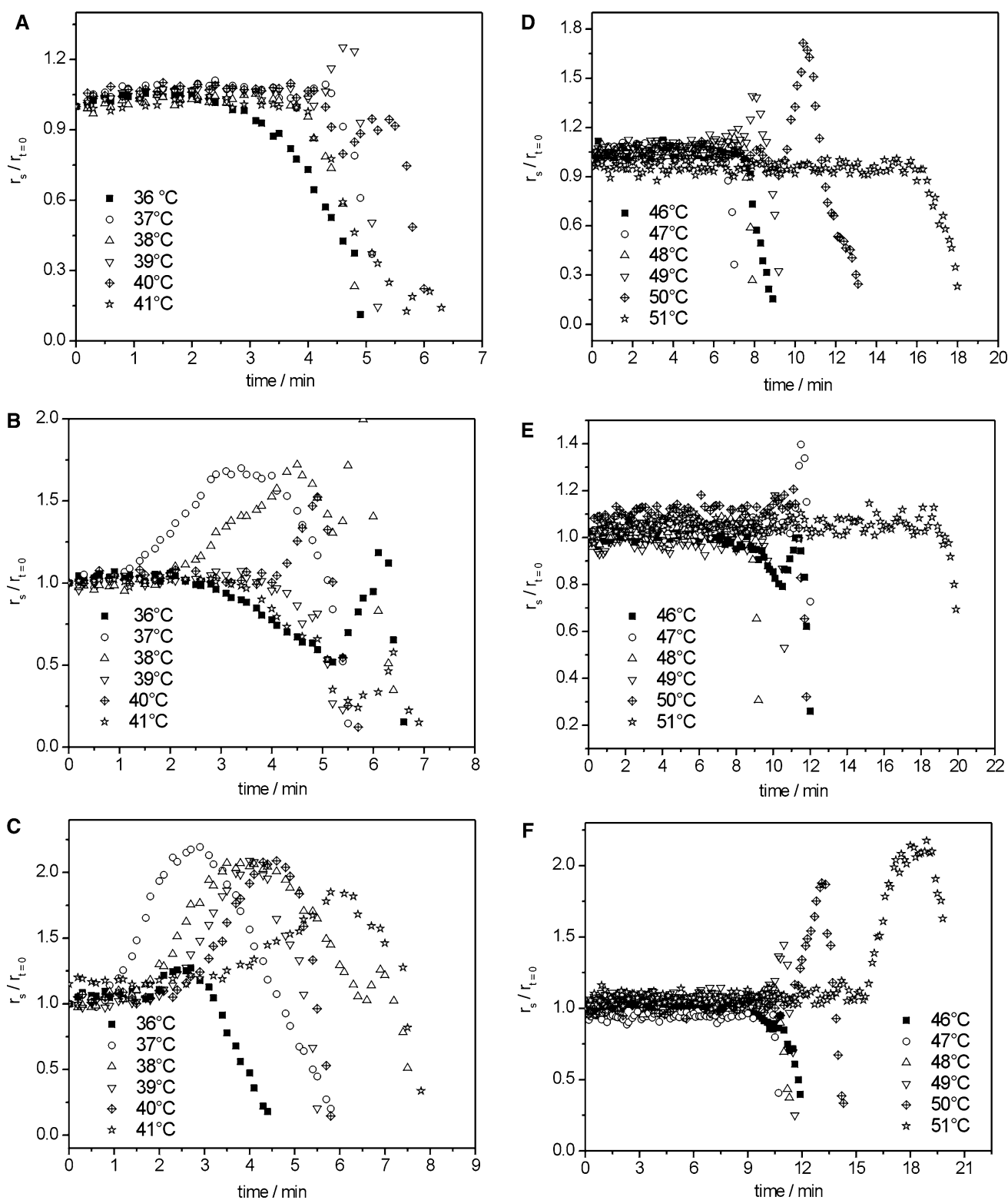


**Fig. 3** Normalized anisotropy as a function of time for **a** TP:TO, **b** TP:HOSfO, **c** TP:SBO, **d** TS:TO, **e** TS:HOSfO and **f** TS:SBO at the temperatures indicated in each figure

493 no particular trend as a function of the type of molecule  
 494 used. Hence, we refer hereon only to the short range vdW  
 495 energy in order to explain our experimental results.

The vdW component of a pure TP system upon mini- 496  
 497  
 498

**Table 4** TAG composition (%w/w) of safflower oil high in triolein (HOSfO) and soybean oil (SBO)

TAG	HOSfO	SBO
LLL	0.48 (0.05)	21.4 (0.5)
LLO OLL	2.24 (0.06)	21.2 (0.9)
LLP	0.26 (0.02)	14.5 (0.6)
LOO	16.20 (0.08)	9.9 (0.1)
PLO POL	1.6 (0.1)	10.42 (0.03)
OOO	65.4 (0.9)	3.67 (0.03)
POO	8.6 (0.3)	2.7 (0.3)

TAGs present in less than a 5% concentration in at least one of the oils have been omitted. Numbers in parentheses correspond to the standard deviation of four measurements

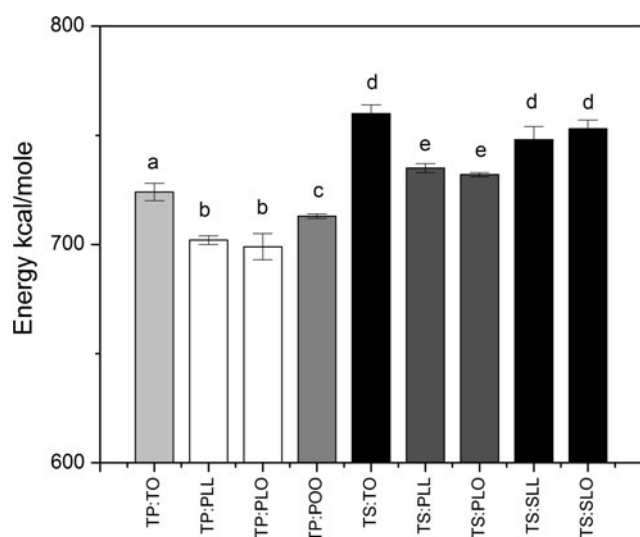


**Fig. 4** Short range vdW interactions for different TAG mixes in a 1:1 M ratio. Error bars correspond to the standard deviation of 3–6 independent simulations with different starting configuration

499 747 ± 2 kcal/mol. This is an indication that vdW forces  
 500 are somehow responsible for the liquid or solid behaviour  
 501 of a TAG. Figure 4 shows the average vdW energy values  
 502 for mixtures of TP:TO, TP:PLL, TP:PLO, TP:POO and the  
 503 analogues in TS blends. PLL in our simulations is com-  
 504 posed of one palmitic and two linoleic acid chains, PLO of  
 505 one palmitic, one linoleic and one oleic acid chain and  
 506 POO of one palmitic and two oleic acid chains. We have  
 507 performed statistical analysis on our results to determine  
 508 which mixes present a potential favorable vdW interaction.  
 509 Also, different initial configurations of the same mix yield  
 510 statistically equivalent results ( $P > 0.05$ ). This then  
 511 allowed for the calculation of an average value for different  
 512 mixes and the determination of statistically significant  
 513 differences between samples. The letters on the bars in  
 514 Fig. 4 summarize our results. In this way, the TP:PLL,  
 515 TP:PLO and TP:POO mixes have a significantly lower

vdW energy than the TP:TO blend. A similar trend is seen  
 516 for the TS:PLL and TS:PLO with respect to the TS:TO  
 517 analogue. The same tendency was seen for mixtures in a  
 518 1:3 stoichiometry (data not shown). The last two bars  
 519 correspond to blends of TS:SLL and TS:SLO. Although  
 520 SLL and SLO exist in very small proportions in the oils, we  
 521 have treated these blends with TS as “hypothetical”. The  
 522 purpose was to prove if the decrease in the vdW energy  
 523 was related to the length of the TAGs involved or due to a  
 524 specific effect related to the presence of palmitic acid in the  
 525 TAG molecule. This last result seems to indicate that  
 526 TAGs containing at least one saturated 16-carbon chain  
 527 interact better with both TP and TS. Hence, the specificity  
 528 does not arise from same length chains in the solute and  
 529 solvent TAGs, but from a particular aspect of the palmitic  
 530 acid.  
 531

## Discussion

532  
 533 This work deals with the behavior of liquid oils in the  
 534 presence of fully saturated TAGs. We have used both TP  
 535 and TS with the purpose of comparing the effect that car-  
 536 bon chain length has on the behavior of the system. When a  
 537 fluid has a preferential motion in a particular dimension or  
 538 has an orientational restriction, it is said that the fluid is  
 539 structured and hence displays anisotropy. This ordering of  
 540 the fluid causes a change in the microviscosity of the  
 541 system. Interestingly enough, this change in the microvis-  
 542 cosity is highly correlated to the bulk viscosity of the  
 543 system. Our fluorescence polarization results clearly indi-  
 544 cate that there is a pre-nucleation structuring of the blend  
 545 characterized by an increase of the anisotropy as a function  
 546 of time as seen in Fig. 3. Our calorimetric data are sup-  
 547 porting evidence that our FPS results are not due to a  
 548 solubility or phase behavior effect, but rather a specific  
 549 interaction of the blend components at the molecular level.  
 550 In this work, we have ran single-component and bi-com-  
 551 ponent MM simulations, to gain a better insight on the  
 552 forces responsible for the pre-nucleation structuring seen in  
 553 the FPS experiments.

554 The energies given by the Chem3D program are not  
 555 related to any thermodynamic quantity, and have no  
 556 meaning as absolute quantities. However, the values can be  
 557 used for comparing relative behaviors between different  
 558 conformations as done in this work. The total energy is  
 559 divided into seven components: stretch, bend, stretch-bend  
 560 combination, torsion, non-1,4 (or long range) van der  
 561 Waals, 1,4 (or short range) van der Waals and dipole/dipole  
 562 interactions. The sum of all these components corresponds  
 563 to the total minimized energy of the system. Since bonded  
 564 interactions are highly dependent on the initial configura-  
 565 tion of the molecule, we have only used the terms

566 corresponding to non bonded interactions in our initial  
567 assessment of the energy minimization. The non-bonded  
568 interactions given by the program correspond to long and  
569 short range van der Waals forces and dipole/dipole inter-  
570 actions. Of these, only the short range vdW interactions  
571 displayed a pattern as a function of the TAG molecule used  
572 in the mix. This is in agreement with the work of Sato et al.  
573 [4] who have suggested that van der Waals interactions are  
574 responsible for the lamellar structure seen in their XRD  
575 measurements on monounsaturated TAGs.

576 For either TP or TS, Fig. 4 clearly indicates that the  
577 vdW energies are highest for mixes with TO. Hence the  
578 interaction between these TAGs is the least favorable.  
579 We believe that this is the reason why our FPS experi-  
580 ments show no increase in the anisotropy for the TO  
581 blends. Simulations for mixes of PLL and PLO with both  
582 saturated fats, show a decrease in the vdW energy with  
583 respect to the TO samples. We have interpreted this as an  
584 indication of a particular behavior occurring in the  
585 presence of TAGs that contain at least one palmitic acid.  
586 This explains the experimental result obtained through  
587 FPS, in which mixtures of TP:HOSfO and TP:SBO  
588 showed an increase in the microviscosity. HOSfO has  
589 about 10% of TAGs containing palmitic acid in their  
590 composition whereas SBO has a content of close to 30%  
591 of these TAGs. We believe that it is the presence and  
592 abundance of these palmitic acid-containing TAGs what  
593 determines the increase in the microviscosity prior to the  
594 actual nucleation of fat crystals. Hence, although an  
595 increase in anisotropy is seen in the TP:HOSfO blends,  
596 the highest effect is seen for the TP:SBO and TS:SBO  
597 samples.

598 Our results suggest that blends of saturated fats in oils  
599 that contain at least 10% of TAGs with at least one chain of  
600 palmitic acid, will show an increase in the microviscosity  
601 as a pre-nucleation step in the crystallization process. One  
602 could now hypothesize that this result is extensible to  
603 longer chain analogues. Hence, to induce crystallization  
604 one needs a liquid oil that has a relatively high content of  
605 TAGs that have at least one saturated chain. Interestingly,  
606 the effect is very specific to palmitic acid. The MM sim-  
607 ulations performed on hypothetical blends of TS:SLL and  
608 TS:SLO indicate that the even if the saturated chain length  
609 is the same as that of the solid fat, the interaction is not  
610 necessarily favorable enough to induce ordering in the pre-  
611 nucleation stage. Very recently, Vereecken et al. [25] have  
612 suggested on the basis of DSC measurements, that TP  
613 seems to play a more important role as seeding agent in the  
614 crystallization of POP than TS does for SOS. This inter-  
615 esting conclusion agrees with the specific behavior seen for  
616 the palmitic-TAGs with respect to the stearic-containing  
617 analogues.

## Conclusions

This work has studied the pre-nucleation ordering occur-  
ing in blends of saturated TAGs in different liquid oils.  
Our FPS experiments have given us insight on the micro-  
scopic level structuring that occurs at this stage. However,  
it was not clear which interactions were responsible for this  
effect at the molecular level. We performed MM simula-  
tions to address this aspect. MM is a fast and simple, yet  
powerful, tool that can provide complementary information  
to experimental data. Obviously, the results obtained need  
to be carefully interpreted based on the conditions used for  
the simulations. Once this is achieved, the resulting out-  
come of this procedure is usually a better understanding of  
the molecular interactions responsible for a particular  
phenomenon observed experimentally. Using MM we have  
been able to determine that van der Waals interactions are  
key in the stage prior to the nucleation of fats. We have  
also shown that a specific behavior occurs depending on  
the molecular composition of a particular TAG. These  
results indicate that both general and specific interactions  
play a role in the pre-nucleation step. It is our hope that this  
work has set grounds for the implementation of MM sim-  
ulations in similar systems to the ones here presented.

## References

1. Freedericksz V, Zolina V (1933) Forces causing the orientation of an anisotropic liquid. *Trans Faraday Soc* 29:919–930
2. Cebula DJ, McClements DJ, Povey MJW, Smith PR (1992) Neutron diffraction studies of liquid and crystalline trilaurin. *J Am Oil Chem Soc* 69:130–136
3. Larsson K (1972) Molecular arrangement in glycerides. *Fette Seifen Anstrichmittel* 74:136
4. Minato A, Ueno S, Smith K, Amemiya Y, Sato K (1997) Thermodynamic and kinetic study on phase behavior of binary mixtures of POP and PPO forming molecular compound systems. *J Phys Chem B* 101:3498–3505
5. Ueno S, Minato A, Yano J, Sato K (1999) Synchrotron radiation x-ray diffraction study of polymorphic crystallization of SOS from liquid phase. *J Cryst Growth* 198:1326–1329
6. Corkery RW, Rousseau D, Smith P, Pink DA, Hanna CB (2007) A case for discotic liquid crystals in molten triglycerides. *Langmuir* 23:7241–7246
7. Larsson K (1992) On the structure of the liquid state of triglycerides. *J Am Oil Chem Soc* 69:835–836
8. Hernqvist L (1984) On the structure of triglycerides in the liquid state and fat crystallization. *Fette Seifen Anstrichmittel* 86:297–300
9. Larsson K (1979) An x-ray scattering study of the L2-phase in monoglyceride-water system. *J Colloid Interface Sci* 72:152–153
10. Toro-Vazquez JF, Gallegos-Infante A (1996) Viscosity and its relationship to crystallization in a binary system of saturated triacylglycerides and sesame seed oil. *J Am Oil Chem Soc* 73:1237–1246
11. Marangoni AG (2002) Steady state fluorescence polarization spectroscopy as a tool to determine microviscosity and structural

- 672 order in lipid systems. In: Marangoni AG, Narine S (eds) Physical  
673 properties of lipids. Marcel Dekker, New York, pp 163–189  
674
- 674 12. Murakami A, Nakaura M, Nakatsuji Y, Nagahara S, Tran-Cong  
675 Q, Makino K (1991) Fluorescent-labeled oligonucleotide probes:  
676 detection of hybrid formation in solution by fluorescence polar-  
677 ization spectroscopy. *Nucleic Acids Res* 19:4097
- 678 13. Parasassi T, De Stasio G, d'Ubaldo A, Gratton E (1990) Phase  
679 fluctuation in phospholipid membranes revealed by Laurdan  
680 fluorescence. *Biophys J* 57:1179–1186
- 681 14. Yguerabide J, Stryer L (1971) Fluorescence spectroscopy of an  
682 oriented model membrane. *PNAS* 68:1217–1221
- 683 15. Royer CA (1995) Fluorescence spectroscopy. *Methods Mol Biol*  
684 40:65–89
- 685 16. Mann TL, Krull UJ (2003) Fluorescence polarization spectros-  
686 copy in protein analysis. *Analyst* 128:313–317
- 687 17. Nagarajan K, Myerson AS (2001) Molecular dynamics of  
688 nucleation and crystallization of polymers. *Cryst Growth Des*  
689 1:131–142
- 690 18. Terrill NJ, Fairclough PA, Towns-Andrews E, Komanschek BU,  
691 Young RJ, Ryan AJ (1998) Density fluctuations: the nucleation  
692 event in isotactic polypropylene crystallization. *Polymer*  
693 39:2381–2385
- 694 19. Perez-Martinez D, Alvarez-Salas C, Charo-Alonso M, Dibildox-  
695 Alvarado E, Toro-Vazquez JF (2007) The cooling rate effect on  
the microstructure and rheological properties of blends of cocoa  
butter with vegetable oils. *Food Res Int* 40:47–62
- 696 20. Kloek W, Walstra P, van Vliet T (2000) Crystallization kinetics  
697 of fully hydrogenated palm oil in sunflower oil mixtures. *J Am*  
698 *Oil Chem Soc* 77:389–398
- 699 21. Lakowicz JR (1999) Fluorescence anisotropy. In: Lakowicz JR  
700 (ed) *Principles of fluorescence spectroscopy*. Plenum Press, New  
701 York, pp 291–319
- 702 22. Allinger NL (1977) Conformational analysis. 130. MM2.  
703 A hydrocarbon force field utilizing V1 and V2 torsional terms.  
704 *JACS* 99:8127–8134
- 705 23. Weber G, Shinitzky M, Dianoux AC, Gitler C (1971) Microvis-  
706 cosity and order in the hydrocarbon region of micelles and  
707 membranes determined with fluorescent probes. I. Synthetic  
708 micelles. *Biochemistry (NY)* 10:2106–2113
- 709 24. Mateo CR, Lillo MP, Brochon JC, Martinez-Ripoll M,  
710 Sanz-Aparicio J, Acuna AU (1993) Rotational dynamics of  
711 1,6-diphenyl-1,3,5-hexatriene and derivatives from fluorescence  
712 depolarization. *J Phys Chem A* 97:3486–3491
- 713 25. Vereecken J, Foubert I, Smith KW, Dewettinck K (2009) Effect  
714 of SatSatSat and SatOSat on crystallization of model fat blends.  
715 *Eur J Lipid Sci Technol* 111:243–258
- 716  
717  
718

UNCORRECTED PROOF

### **III. RESUMEN EN EXTENSO Y SEGUNDO ARTÍCULO**

## **Estructuración Previa a la Nucleación de Triacilgliceroles y su Efecto Sobre la Energía de Activación para la Nucleación**

Elena Dibildox-Alvarado<sup>1</sup>, Alejandro G. Marangoni<sup>2</sup>, Jorge F. Toro-Vazquez<sup>3</sup>

<sup>1</sup>Universidad Autónoma de Querétaro, DIPA-PROPAC, México. <sup>2</sup>University of Guelph, Department of Food Science, Guelph, Canadá <sup>3</sup>Universidad Autónoma de San Luis Potosí, Facultad de Ciencias Químicas, México.

### **RESUMEN**

Basados en un estudio previo que involucró mediciones de anisotropía ( $r_s$ ) y simulación mecánica molecular (MM), en el presente trabajo fue investigada la interacción molecular producida entre los triacilgliceroles (TAGs) antes de su nucleación y su posible participación en la determinación de la energía libre de activación necesaria para desarrollar un núcleo estable ( $\Delta G_c$ ). La ecuación de Fisher-Turnbull fue utilizada para calcular la  $\Delta G_c$  implicada en la nucleación de la tripalmitina (TP) o la triestearina (TS) mezcladas en una proporción 25:75 con trioleína (TO), aceite de cártamo alto en oleico (HOSfO) y aceite de soya (SBO). Las temperaturas de cristalización y fusión correspondientes así como los tiempos de inducción a la cristalización fueron determinados por calorimetría diferencial de barrido. Basados en los valores de la temperatura de fusión en el equilibrio ( $T_M^\circ$ ), las temperaturas de cristalización ( $T_{Cr}$ ) utilizadas fueron seleccionadas para obtener condiciones de superenfriamiento similares en todas las mezclas de TP y TS investigadas. Así, el superenfriamiento fue calculado como  $T_M^\circ - T_{Cr}$ . Para las mezclas de TP, el tiempo de inducción a la cristalización ( $t_i$ ) fue medido desde 36 °C hasta 41 °C cada grado y, para las mezclas

de TS desde 46 °C hasta 51 °C cada grado. Los resultados fueron estadísticamente analizados por ANOVA (Statistica, V 9.0) contrastando las medias de los tratamientos. Por otro lado, la anisotropía de las mezclas fue determinada durante las etapas de enfriamiento e isotérmica, con un espectrofotómetro de fluorescencia polarizada empleando los mismos patrones tiempo-temperatura que para las mediciones de  $t_i$ . La  $r_s$  para las diferentes mezclas de TP y TS fue graficada en función de  $T_M^\circ - T_{Cr}$ .

Las  $T_M^\circ$  para la TP y TS en sus tres mezclas fueron 59.7°C ( $\pm 0.83$ ) y 70.2°C ( $\pm 0.27$ ) respectivamente, ya que resultaron ser independientes del tipo de disolvente. Por otro lado, los correspondientes  $t_i$  y  $\Delta G_c$  en función del superenfriamiento para las mezclas de TP y TS son mostrados respectivamente en las Tablas 1 y 2. A todas las  $T_{Cr}$  fue siempre obtenida una exoterma simple de cristalización que correspondió al polimorfo  $\beta$  para la TP o TS cristalizada en las mezclas. La regresión lineal del  $\log[(t_i)(T_{Cr})]$  vs.  $1/T_{Cr}(T_M^\circ - T_{Cr})^2$  dio en todos los casos coeficientes de determinación ( $R^2$ ) mayores a 0.86 (ej.,  $R > 0.927$ ). Como ejemplo, la figura 1 incluye las gráficas Fisher-Turnbull para las mezclas de TP (Fig. 1a) y de TS (Fig. 1b).

En general, para todas las muestras investigadas, el  $t_i$  y la  $\Delta G_c$  incrementaron a medida que el superenfriamiento disminuyó. En todos los casos, para un superenfriamiento similar,  $t_i$  fue mayor en las mezclas de TS que en las mezclas de TP. Para las mezclas de TP a todos los niveles de superenfriamiento investigados, el  $t_i$  mayor fue para las mezclas TP/SBO (Tabla 1) mientras que la  $\Delta G_c$  se vio incrementada siguiendo el orden SBO>HOSfO>TO (Tabla 2). Sin embargo, se hace notar que la  $\Delta G_c$  para las mezclas de TP/SBO y TP/HOSfO no fue estadísticamente diferente a ninguna de las  $T_{Cr}$  investigadas ( $P=0.12$ ; Tabla 2). En contraste, el  $t_i$  en las mezclas de TS no mostró una



tendencia en particular y  $\Delta G_c$  se incrementó siguiendo el orden TO>SBO>HOSfO. Esto indicó, que sobre condiciones similares de superenfriamiento, la TP requirió más energía para nuclear en el SBO y el HOSfO que en la TO, mientras que la nucleación de la TS requirió más energía de activación en la TO que en SBO y HOSfO.

Nuestros estudios previos que involucraron mediciones de anisotropía y simulación MM mostraron que la presencia de moléculas de TAGS conteniendo al menos una cadena de ácido palmítico en su estructura es un requisito para inducir una interacción molecular a través de fuerzas van der Waals (vdW) con la TP y TS y por lo tanto promover una estructuración previa a la nucleación de TAGS. De acuerdo a la composición de TAGS previamente reportada, el ácido palmítico no estuvo presente en la trioleína y sí en los aceites de soya y alto oleico como LLP, PLO, POL and, POO. Entonces, la presencia de TAGS conteniendo ácido palmítico en las mezclas hechas con HOSfO y SBO debería inducir una estructuración de TAGS previo a la nucleación. Comparando la  $\Delta G_c$  para las mezclas hechas con TO, resulta un alto requerimiento de energía para la nucleación de la TP en las mezclas hechas con HOSfO y SBO. En contraste, la nucleación de la TS en HOSfO y SBO requirió menos energía que mezclada con TO.

Por otro lado, la organización de los TAGS en las mezclas investigadas pudo ser evaluada por la evolución de  $r_s$  mientras el sistema fue enfriado hasta alcanzar las condiciones isotérmicas para la cristalización. Así, la figura 2 muestra el comportamiento de la  $r_s$  de las mezclas en función del superenfriamiento durante la etapa de enfriamiento y el inicio de la cristalización isotérmica. Durante la etapa de enfriamiento, todas las mezclas investigadas mostraron un incremento exponencial de la  $r_s$  a medida que el superenfriamiento aumentó (Fig. 2). Sin embargo, se apreciaron los siguientes comportamientos. Todas las mezclas de TP observaron valores similares

de  $r_s$  y su cambio fue independiente del tipo de mezcla (ej., las tres mezclas presentaron la misma ecuación de ajuste). En el mismo contexto, los TAGS en el estado líquido fueron más estructurados en las mezclas de TP que en las mezclas TS (ej., todas las muestras de TS mostraron valores menores de  $r_s$  que las muestras de TP. Adicionalmente, en las mezclas de TS los valores de  $r_s$  mostraron el siguiente orden TO>HOSfO>SBO. Sin embargo, como se observó para  $\Delta G_{cr}$ , los valores de  $r_s$  para TS/SBO y TS/HOSfO no fueron estadísticamente diferentes.

Con lo anterior se concluye que durante la etapa de enfriamiento, la adición de TP a la TO, HOSfO y SBO no modifica la estructura original de los TAGS. En contraste, la adición de TS resulta en una disminución de la estructura de los TAGS líquidos particularmente en las mezclas TS/HOSfO y TS/SBO. Debido a que la mezcla TS/TO no mostró cambio en la pendiente (Fig. 2), la estructuración de los TAGS en la fase líquida no fue asociada a la trioleína.

De acuerdo al análisis de TAGS previamente reportado, el HOSfO presentó cerca de un 10% de TAGS conteniendo ácido palmítico en su composición mientras que el SBO tuvo aproximadamente 30% de estos TAGS. Entonces, los valores bajos de  $r_s$  observados en las muestras de TS en HOSfO y SBO comparados con los observados en TO, pueden estar asociados a la concentración de TAGS con ácido palmítico presentes en la mezcla.

La figura 3 muestra la evolución de la  $r_s$  bajo condiciones isotérmicas para diferentes mezclas de TP y TS. Una vez bajo estas condiciones, los valores de la  $r_s$  en todas las mezclas de TS permanecieron constantes en función del tiempo hasta que fue alcanzado el  $t_i$ . Este comportamiento fue observado a todas las  $T_{Cr}$  investigadas y, como ejemplo se muestra en la figura 3c la mezcla de TS/SBO cristalizada a 48 °C y 50 °C. El decremento en  $r_s$  observado

después de la nucleación (ej., después de  $t_i$ ) fue asociado a la dispersión de la luz por los núcleos desarrollados. En contraste a las mezclas de TS, las mezclas TP/HOSfO y TP/SBO mostraron un incremento en la  $r_s$  en función del tiempo, este aumento fue en función directa del contenido de TAGS con al menos una cadena ácido palmítico y siguiendo el orden TP/SBO > TP/HOSfO. Así, las interacciones moleculares de la TP con POO, LLP y PLO/POL fueron tanto tiempo como temperatura dependientes y al parecer dificultaron la nucleación de la TP, ya que la  $\Delta G_c$  fue mayor en las mezclas TP/SBO y TP/HOSfO comparada con la  $\Delta G_c$  de la mezcla TP/TO (Tabla 2).

Otros investigadores han mostrado que mezclas de TP y POO cristalizan más lentamente que los TAGS puros, esto a pesar de que la TP y el POO observaron una cristalización independiente. Entonces, probablemente las interacciones moleculares que ocurrieron en la fase líquida entre la TP y los TAGS con ácido palmítico resultaron en el desarrollo de una estructura líquida lamelar de TAGS mixtos. Esto podría retrasar el proceso de nucleación hasta que la TP fuera segregada de dicha estructura lamelar. El resultado fue una mayor  $\Delta G_c$  requerida para la nucleación de la TP en el sistema a medida que la concentración de TAGS con ácido palmítico (ej., LLP, POO y PLO/POL) aumenta en las mezclas.

1 Food Biophysics  
2 DOI 10.1007/s11483-010-9163-2

3 ORIGINAL ARTICLE

## 4 Pre-nucleation Structuring of Triacylglycerols and Its Effect 5 on the Activation Energy of Nucleation

6 Elena Dibildox-Alvarado · Alejandro G. Marangoni ·  
7 Jorge F. Toro-Vazquez

8  
9 © Springer Science+Business Media, LLC 2010

11 **Abstract** Based in a previous study involving anisotropy  
12 measurements ( $r_s$ ) and molecular mechanics simulations,  
13 we investigated the molecular interaction occurring among  
14 triacylglycerols (TAGS) before their nucleation, and its  
15 possible involvement in determining the activation free  
16 energy to develop a stable nucleus ( $\Delta G_c$ ). The Fisher-  
17 Turnbull equation was used to calculate the  $\Delta G_c$  involved  
18 in the nucleation of tripalmitin (TP) or tristearin (TS)  
19 blended in a 25:75 ratio with triolein (TO), high oleic  
20 safflower oil (HOSfO), and soybean oil (SBO). The  
21 crystallization temperatures used were selected to obtain  
22 similar supercooling conditions in all blends investigated.  
23 As our previous study showed, the anisotropy measure-  
24 ments ( $r_s$ ) showed that TAGS with at least one chain of  
25 palmitic acid (i.e., POO, LLP, PLO) induce TAGS' pre-  
26 nucleation structuring in both the TP and TS blends.  
27 However, for TS blends, the molecular interaction occurred  
28 well before attaining supercooling conditions required for  
29 crystallization (i.e., during the cooling stage). Once these

supercooling conditions were achieved, TAGS with pal- 30  
mitic acid acted as template for TS crystallization. As a 31  
result,  $\Delta G_c$  in TS/HOSfO and TS/SBO blends were lower 32  
than the  $\Delta G_c$  in the TS/TO blend. In contrast, in the TP 33  
blends TAGS structuring (i.e., an increase in  $r_s$ ) occurred as 34  
a function of time under isothermal conditions as a direct 35  
function of the concentration of TAGS containing at least 36  
one chain of palmitic acid. We postulate that the molecular 37  
interactions occurring in the liquid phase between TP and 38  
TAGS with palmitic acid, resulted in the development of a 39  
mixed TAGS lamellar liquid structure. This delayed TP 40  
nucleation until segregation of TP from the mixed TAGS 41  
lamellar liquid structure occurred. This resulted in a higher 42  
 $\Delta G_c$  for TP nucleation as the concentration of LLP, POO, 43  
PLO, and PLO increased in the blends. The molecular 44  
interactions occurring among TAGS in the liquid phase 45  
under supercooling conditions must be understood, since 46  
they directly relate to the TAGS crystallization process that 47  
in turns determines the macroscopic properties evaluated by 48  
consumer in lipid-based products. The results presented in 49  
this manuscript are in this line of investigation. 50

E. Dibildox-Alvarado · J. F. Toro-Vazquez  
Universidad Autonoma de San Luis Potosi,  
Facultad de Ciencias Quimicas,  
San Luis Potosi, Mexico

E. Dibildox-Alvarado  
Universidad Autonoma de Queretaro, DIPA-PROPAC,  
Santiago de Querétaro, Mexico

A. G. Marangoni  
University of Guelph, Department of Food Science,  
Guelph, Canada

J. F. Toro-Vazquez (✉)  
Facultad de Ciencias Quimicas-CIEP,  
Av. Dr. Manuel Nava 6, Zona Universitaria,  
San Luis Potosí, SLP 78210, Mexico  
e-mail: toro@uaslp.mx

**Keywords** Pre-nucleation structuring · Triacylglycerols 51  
structuring · Fisher-Turnbull · Anisotropy · 52  
Triacylglycerols nucleation 53

**Introduction** 54

Vegetable oils and fats are multicomponent systems con- 55  
taining different families of triacylglycerols (TAGS). In 56  
these systems, the molecular relationships occurring among 57  
TAGS families determine the thermodynamic conditions 58  
(i.e., supercooling and supersaturation) that drive the 59  
formation of a solid from the liquid phase, the organization 60

61 of the solid phase, and its phase behavior. The resulting  
62 three-dimensional TAGS crystal network and the phase  
63 behavior of TAGS are major factors determining the  
64 physical and functional properties (i.e., rheology, liquid  
65 phase entrapment, mouthfeel, appearance, and spread-  
66 ability) in products such as margarine, butter, confec-  
67 tionary coatings, and fillings<sup>1</sup>. Thus, the complex  
68 molecular interactions occurring among TAGS in the  
69 liquid phase under supercooling conditions must be first  
70 understood, since they directly relate to the TAGS  
71 crystallization process that in turns determines the macro-  
72 scopic properties evaluated by consumer in vegetable oil  
73 and fat-based products.

74 Nematic<sup>2</sup>, smectic<sup>3</sup>, and discotic<sup>4</sup> phases have been  
75 proposed as the structural molecular arrangement for  
76 TAGS in the liquid phase. Although the actual structural  
77 mesophase organization of TAGS has not been estab-  
78 lished, all the work mentioned above agrees on the fact  
79 that TAGS molecules are somehow structured in a liquid  
80 crystalline-like state. Recently, we reported the pre-  
81 nucleation behavior of tripalmitin (TP) and tristearin  
82 (TS) in blends with triolein (TO), high oleic safflower  
83 oil (HOSfO), and soybean oil (SBO) as evaluated through  
84 anisotropy measurements and molecular mechanics simu-  
85 lations<sup>5</sup>. The TP/HOSfO and TP/SBO blends showed an  
86 increase in anisotropy, a behavior directly associated to an  
87 increase in the microviscosity of the blend that we  
88 interpreted as a structuring of TAGS before nucleation  
89 and growth of the crystals. A similar but less pronounced  
90 effect was also observed in the TS/SBO blends, but here  
91 the increase in anisotropy occurred after nucleation. This  
92 behavior was not observed in the TP/TO and the TS/TO  
93 blends<sup>5</sup>. We performed molecular mechanics simulations  
94 in an attempt to understand the molecular interactions  
95 responsible for this behavior. The simulation results  
96 indicated that the presence of TAGS molecules containing  
97 at least one chain of palmitic acid is a requisite to induce a  
98 molecular interaction through van der Waals forces with  
99 TP or TS, and therefore a pre-nucleation structuring of  
100 TAGS with the subsequent increase in the anisotropy, and  
101 therefore, in the microviscosity of the blends.

102 Within this framework, we investigated the molecular  
103 interaction occurring among TAGS before their nucleation,  
104 and its possible involvement in determining the activation  
105 free energy to develop a stable nucleus ( $\Delta G_c$ ). As in our  
106 previous study<sup>5</sup>, the same TP and TS blends with TO,  
107 HOSfO, and SBO were used in the present investigation.  
108 The Fisher-Turnbull equation was utilized to calculate the  
109  $\Delta G_c$  using the induction time of crystallization ( $t_i$ ) of the  
110 blends determined by differential scanning calorimetry  
111 (DSC) at different crystallization temperatures. To under-  
112 stand the behavior of  $\Delta G_c$  in the blends, we performed an  
113 additional analysis of the anisotropy behavior in the blends

114 to the one already done in our previous study<sup>5</sup>. The  
115 crystallization temperatures were selected in such a way to  
116 obtain similar supercooling conditions in all the blends  
117 investigated. As previously indicated<sup>5</sup>, the blends investi-  
118 gated provided different degrees of molecular compatibil-  
119 ity among the saturated TAGS (i.e., TP or TS) and the  
120 TAGS present in TO, HOSfO, and SBO. This since, in TO  
121 the major TAGS present was OOO (>99%), while in  
122 HOSfO were mainly OOO ( $\approx 66\%$ ), OOL ( $\approx 16\%$ ), POO  
123 ( $\approx 8.7\%$ ), and PLO ( $\approx 1.6\%$ ), and in SBO  $\approx 56\%$  of TAGS  
124 were OOO, OOL, LLL, and LLO and  $\approx 27\%$  were POO,  
125 PLO, and LLP (where O=oleic acid, L=linoleic acid, and  
126 P=palmitic acid).

## Materials and Methods 127

### Blends Preparation 128

129 The TAGS, i.e., TP, TS, and TO, with purity higher than  
130 99% were obtained from Sigma Chemical Co. (St. Louis,  
131 MO, USA). The HOSfO and the SBO were obtained from  
132 local manufacturers, their main TAGS composition has  
133 been reported previously<sup>5</sup>. Blends of each of the saturated  
134 TAGS (i.e., TP and TS) in TO, HOSfO, and SBO were  
135 prepared in a 25:75 (wt/wt) ratio as previously described<sup>5</sup>.

### Isothermal Crystallization 136

137 Based on dynamic thermograms obtained by DSC with a TA  
138 Instruments Model Q2000 (TA Instruments, New Castle,  
139 Delaware, USA) as described previously<sup>5</sup>, different crystalli-  
140 zation temperatures were established for isothermal crystal-  
141 lization studies. Thus, blend samples (6–8 mg) sealed in  
142 aluminum pans were heated (80°C/20 min) and then cooled  
143 to the corresponding crystallization temperature at 10°C/min.  
144 For each crystallized blend the melting temperature at the  
145 peak ( $T_M'$ ) was calculated with the equipment software using  
146 the first derivative of the heat flux<sup>6</sup>. With the  $T_M'$  values, the  
147 equilibrium melting temperature ( $T_M^\circ$ ) for TP and TS in the  
148 blends was determined following the procedure of Hoffman  
149 and Weeks<sup>7</sup>, as described by Perez-Martinez et al.<sup>8</sup> and Toro-  
150 Vazquez et al.<sup>9</sup>. Based on the  $T_M^\circ$  values, crystallization  
151 temperatures ( $T_{Cr}$ ) were selected in such a way to obtain  
152 similar supercooling conditions for all TP and TS blends  
153 investigated. The supercooling was calculated as  $T_M^\circ - T_{Cr}$ .  
154 At each  $T_{Cr}$ , the induction time of crystallization ( $t_i$ ) was  
155 determined with the equipment software using the first  
156 derivative of the heat flux. For the TP blends, the  $t_i$  was  
157 measured from 36°C to 41°C every degree, and for the TS  
158 blends from 46°C to 51°C every degree. In all cases, at least  
159 three independent determinations were obtained. The results  
160 were analyzed through ANOVA and contrast among the

161 treatment means using STATISTICA (V 9.0; StatSoft Inc.,  
162 Tulsa, OK, USA).

163 Determination of  $\Delta G_c$

164 The Fisher-Turnbull equation was utilized to determine  
165 the magnitude of  $\Delta G_c$  for the TP and the TS blends at  
166 each  $T_{Cr}$  investigated. The corresponding  $\Delta G_c$  was  
167 calculated according to Ng<sup>10</sup> and Toro-Vazquez et al.<sup>9</sup>  
168 from the slope ( $s$ ) of the linear regression of  $\log[(t_i/T_{Cr})]$   
169 vs.  $1/T_{Cr}(T_M^\circ - T_{Cr})^2$  through the following equation:

$$\Delta G_c = sk / (T_M^\circ - T_{Cr})^2$$

170 where,  $k$  is the Boltzmann constant. The results were  
172 statistically analyzed as in “Isothermal Crystallization”  
173 section.

174 Anisotropy Measurements

175 The anisotropy ( $r_s$ ) of the blends was determined under the  
176 cooling and isothermal stages of the blends crystallization  
177 with a polarizer spectrophotometer (MD-5020 of Photon  
178 Technology International, London, ON, Canada) using the  
179 same time temperature as for  $t_i$  measurements (see  
180 “Isothermal Crystallization” section). We have described  
181 the details of the determination previously<sup>5</sup>. The  $r_s$  for the  
182 different TP and TS blends were plotted as a function of  
183  $T_M^\circ - T_{Cr}$ .

**Results and Discussion**

184

$t_i$  and  $\Delta G_c$  Analysis

185

The  $T_M^\circ$  for TP and TS in the three blends was 59.7°C  
(±0.83°C) and 70.2°C (±0.27°C), respectively (i.e.,  $T_M^\circ$  for  
TP and TS was independent of the type of blend). As stated  
in the “Material and Methods” section, the  $T_{Cr}$ s selected for  
the isothermal crystallization studies provided similar super-  
cooling (i.e.,  $T_M^\circ - T_{Cr}$ ) conditions for TP and TS blends.  
Supercooling as calculated in the present manuscript, and  
supersaturation [ $\ln(\beta)$ ] calculated as in our previous paper<sup>5</sup>  
(i.e., from the equality between the chemical potential  
equation and the Hildebrand equation), provided values of  
different magnitude but both measurements were highly  
correlated (Tables 1 and 2;  $R^2 > 0.9830$ ,  $P < 0.001$ ).

186  
187  
188  
189  
190  
191  
192  
193  
194  
195  
196  
197

The corresponding  $t_i$  and  $\Delta G_c$  for the TP and TS blends  
as a function of supercooling are shown in Tables 1 and 2,  
respectively. At any given  $T_{Cr}$ , a single crystallization  
exotherm was always obtained that corresponded to the  $\beta$   
polymorph for TP or TS crystallized in the blends (data not  
shown). X-ray analysis done to the blends<sup>5</sup> showed that at  
all  $T_{Cr}$ s investigated TP and TS crystallized in the  $\beta$   
polymorph (i.e., all diffractograms showed the characteris-  
tic peaks at  $\approx 20$ ,  $\approx 23$ , and  $\approx 24$   $2\theta$  corresponding to the 4.6,  
3.85, and 3.70 Å short spacings of the  $\beta$  polymorph). The  
linear regression of  $\log[(t_i/T_{Cr})]$  vs.  $1/T_{Cr}(T_M^\circ - T_{Cr})^2$   
provided in all cases determination coefficients ( $R^2$ ) greater  
than 0.86 (i.e.,  $R > 0.927$ ). As an example, Figure 1 includes

198  
199  
200  
201  
202  
203  
204  
205  
206  
207  
208  
209  
210

t1.1 **Table 1** Induction time by DSC ( $t_i$ , min) at different supercooling ( $T_M^\circ - T_{Cr}$ ) used in the 25:75 (wt/wt) blends of tripalmitin (TP) or tristearin (TS) with triolein (TO), safflower oil high in triolein (HOSfO), or soybean oil (SBO)

t1.2	$(T_M^\circ - T_{Cr}) \ln(\beta)$	TP <sup>a</sup>			$(T_M^\circ - T_{Cr}) \ln(\beta)$	TS <sup>a</sup>		
		TO	HOSfO	SBO		TO	HOSfO	SBO
t1.3								
t1.4	23.7	2.04a	2.26a	2.08a	24.2	3.56a	4.76b	3.80a
t1.5	0.26	0.04	0.09	0.05	0.24	0.47	0.25	0.72
t1.6	22.7	2.50a	2.04a	2.85b	23.2	4.97a	5.08a	5.42a
t1.7	0.24	0.08	0.14	0.47	0.22	0.45	0.20	0.13
t1.8	21.7	2.66a	2.52a	3.30b	22.2	4.88a	5.73a	6.06b
t1.9	0.22	0.10	0.31	0.05	0.21	0.27	0.35	0.28
t1.10	20.7	2.61a	2.90b	3.70c	21.2	5.56a	5.42a	5.86a
t1.11	0.21	0.20	0.00	0.25	0.19	0.06	1.33	0.48
t1.12	19.7	2.98a	4.01b	4.48c	20.2	8.47a	6.64b	6.34b
t1.13	0.19	0.15	0.19	0.63	0.17	0.34	0.34	0.06
t1.14	18.7	4.79a	4.24a	5.09b	19.2	7.84a	8.14a	9.19b
t1.15	0.18	0.62	0.18	0.61	0.17	1.24	0.82	0.21

The  $\ln(\beta)$  is the prevailing supersaturation as calculated by Dibildox et al.<sup>2</sup>

For the systems with TP or TS at the same  $T_M^\circ - T_{Cr}$ , values with a different letter are statistically different ( $P < 0.10$ ). Values with the same letter are statistically the same

<sup>a</sup> Values are shown as the mean and standard deviation of at least two independent measurements

**Table 2** Free energy for nucleation ( $\Delta G_c$ ) at different supercooling ( $T_M^\circ - T_{Cr}$ ) used in the 25:75 (wt/wt) blends of tripalmitin (TP) or tristearin (TS) with triolein (TO), safflower oil high in triolein (HOSfO), or soybean oil (SBO)

	$(T_M^\circ - T_{Cr}) \text{ Ln}(\beta)$	TP <sup>a</sup>			$(T_M^\circ - T_{Cr}) \text{ Ln}(\beta)$	TS <sup>a</sup>		
		TO	HOSfO	SBO		TO	HOSfO	SBO
t2.1	23.7	1.07a	1.48b	1.64b	24.2	2.01a	1.19b	1.67b
t2.2	0.26	0.29	0.09	0.20	0.24	0.27	0.17	0.34
t2.3	22.7	1.16a	1.61b	1.79b	23.2	2.19a	1.30b	1.82b
t2.4	0.24	0.32	0.10	0.22	0.22	0.30	0.19	0.37
t2.5	21.7	1.27a	1.76b	1.96b	22.2	2.39a	1.42b	1.98b
t2.6	0.22	0.35	0.11	0.24	0.21	0.33	0.20	0.40
t2.7	20.7	1.40a	1.94b	2.15b	21.2	2.62a	1.55b	2.17b
t2.8	0.21	0.38	0.12	0.27	0.19	0.36	0.22	0.44
t2.9	19.7	1.54a	2.14b	2.38b	20.2	2.88a	1.71b	2.40b
t2.10	0.19	0.42	0.13	0.29	0.17	0.39	0.25	0.49
t2.11	18.7	1.71a	2.37b	2.64b	19.2	3.19a	1.89b	2.65b
t2.12	0.18	0.47	0.14	0.33	0.17	0.44	0.27	0.54

The Ln ( $\beta$ ) is the prevailing supersaturation as calculated by Dibildox et al. <sup>2</sup>

<sup>a</sup> Values are shown as the mean and standard deviation of at least two independent measurements

For the systems with TP or TS at the same  $T_M^\circ - T_{Cr}$ , values with a different letter are statistically different ( $P < 0.10$ ). Values with the same letter are statistically the same

211 Fisher-Turnbull plots for TP (Figure 1a) and TS (Figure 1b) 240  
 212 blends, showing the corresponding  $R^2$  and statistical 241  
 213 significance of the regression equation. Thus, as has been 242  
 214 shown by other authors <sup>9-13</sup>, the Fisher-Turnbull equation, 243  
 215 although originally developed for a single-component 244  
 216 system, is applicable to complex TAGS systems as the TP 245  
 217 and TS blends investigated. 246

218 Overall, for all blends investigated,  $t_i$  and  $\Delta G_c$  increased 247  
 219 as supercooling decreased (i.e.,  $T_{Cr}$  increased). In general, 248  
 220 for similar supercooling (and saturation),  $t_i$  was longer for 249  
 221 TS blends than for TP blends. Thus, other factors besides 250  
 222 supercooling must be considered to explain differences in 251  
 223 the crystallization kinetics between homogenous saturated 252  
 224 TAGS (i.e., TP vs. TS). For the TP blends and at all levels 253  
 225 of supercooling investigated,  $t_i$  in the TP/SBO blend was 254  
 226 the longest (Table 1) and  $\Delta G_c$  increased following the order 255  
 227 SBO > HOSfO > TO (Table 2). However, the  $\Delta G_c$  for 256  
 228 TP/SBO and TP/HOSfO blends were not statistically 257  
 229 different at any of the  $T_{Cr}$  investigated ( $P = 0.25$ ; Table 2). 258  
 230 In contrast,  $t_i$  in the TS blends did not show a particular 259  
 231 trend and  $\Delta G_c$  increased following the order TO > SBO > 260  
 232 HOSfO. However, as observed in the TP blends,  $\Delta G_c$  for 261  
 233 TS/SBO and TS/HOSfO blends were not statistically 262  
 234 different ( $P = 0.12$ ; Table 2). This indicated that under similar 263  
 235 supercooling conditions, TP required more energy to nucleate 264  
 236 in SBO and HOSfO than in TO, while TS nucleation required 265  
 237 more activation energy in TO than in SBO and HOSfO. 266  
 238 Within this framework, it is important to point out that in TO,  
 239 the TS nucleation required approximately twice the activation

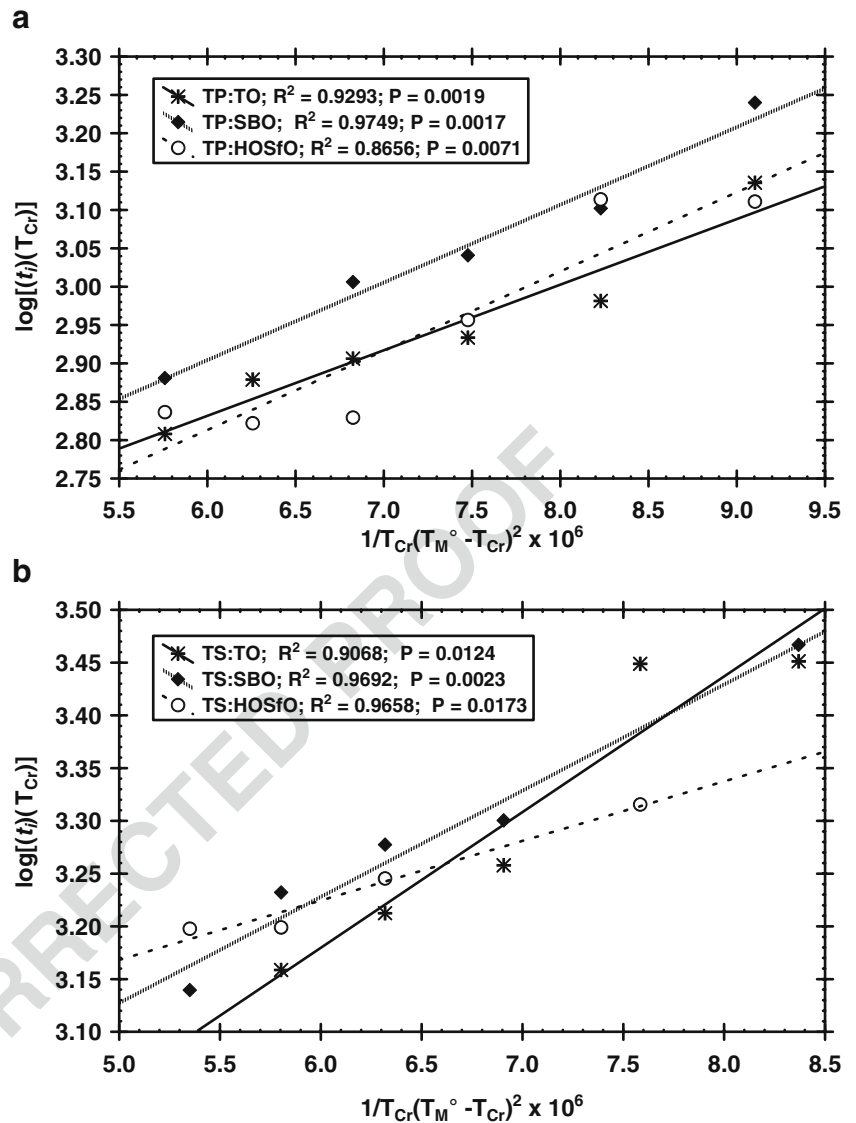
energy than TP, while when blended with SBO and HOSfO, 240  
 both TP and TS showed similar  $\Delta G_c$  values. 241

242 Our previous study involving anisotropy and molecular 243  
 244 mechanics simulations using the same blends<sup>5</sup> showed that the 245  
 246 presence of TAGS molecules containing at least one chain of 246  
 247 palmitic acid (i.e., POO) is a requisite to induce a molecular 247  
 248 interaction through van der Waals forces with TP or TS, and 248  
 249 therefore a pre-nucleation structuring of TAGS. According to 249  
 250 the TAGS composition previously reported<sup>5</sup>, no palmitic acid 250  
 251 was present in TO, while palmitic acid was present in HOSfO 251  
 252 and in SBO as LLP, PLO/POL, and POO. Then, the presence 252  
 253 of TAGS containing palmitic acid in the blends made with 253  
 254 HOSfO and SBO ought to induce a pre-nucleation structuring 254  
 255 of TAGS. Comparing the  $\Delta G_c$  for the blends made with TO, 255  
 256 the TAGS structuring occurring before nucleation (i.e., in the 256  
 257 liquid state) resulted in a higher energy requirement for TP 257  
 258 nucleation in the blends made with HOSfO and SBO 258  
 (Table 2). In contrast, TS nucleation in HOSfO and SBO 259  
 required a lower  $\Delta G_c$  than in the TS/TO blend. 260

Anisotropy Behavior under Cooling and Isothermal 259  
 Conditions 260

261 The organization of TAGS in the blends might be evaluated 261  
 262 by the evolution of  $r_s$  as the system is cooled to achieve 262  
 263 isothermal conditions. The development and attainment of 263  
 264 critical number of TAGS molecules structured in a liquid 264  
 265 state or mesophase is a requirement to achieve TAGS 265  
 266 nucleation. All the works associated with proposing molecular 266

**Fig. 1** Fisher-Tumbull plots for TP (a) and TS (b) blends with TO, HOSfO, and SBO. The legend shows the corresponding determination coefficient ( $R^2$ ) and statistical significance ( $P$ ) of the linear regression equation



267 arrangements for TAGS melts agrees on this<sup>2-4, 14-17</sup>. In fact,  
 268 the change in TAGS viscosity with temperature is  
 269 determined by the shape and size of the TAGS liquid  
 270 structures<sup>18</sup> that is indirectly measured by  $r_s$ . Within this  
 271 framework, in an attempt to understand the behavior of  $\Delta G_c$   
 272 in the blends, Figure 2 shows the behavior of  $r_s$  in the blends  
 273 as a function of supercooling during the cooling and  
 274 isothermal stages. The  $r_s$  value for the isothermal stage  
 275 plotted in Figure 3 was obtained once  $T_{Cr}$  was attained and  
 276 corresponds to the average of  $r_s$  values obtained during the  
 277 first 60 s under isothermal conditions (i.e., before  $t_i$  was  
 278 achieved in the blend).

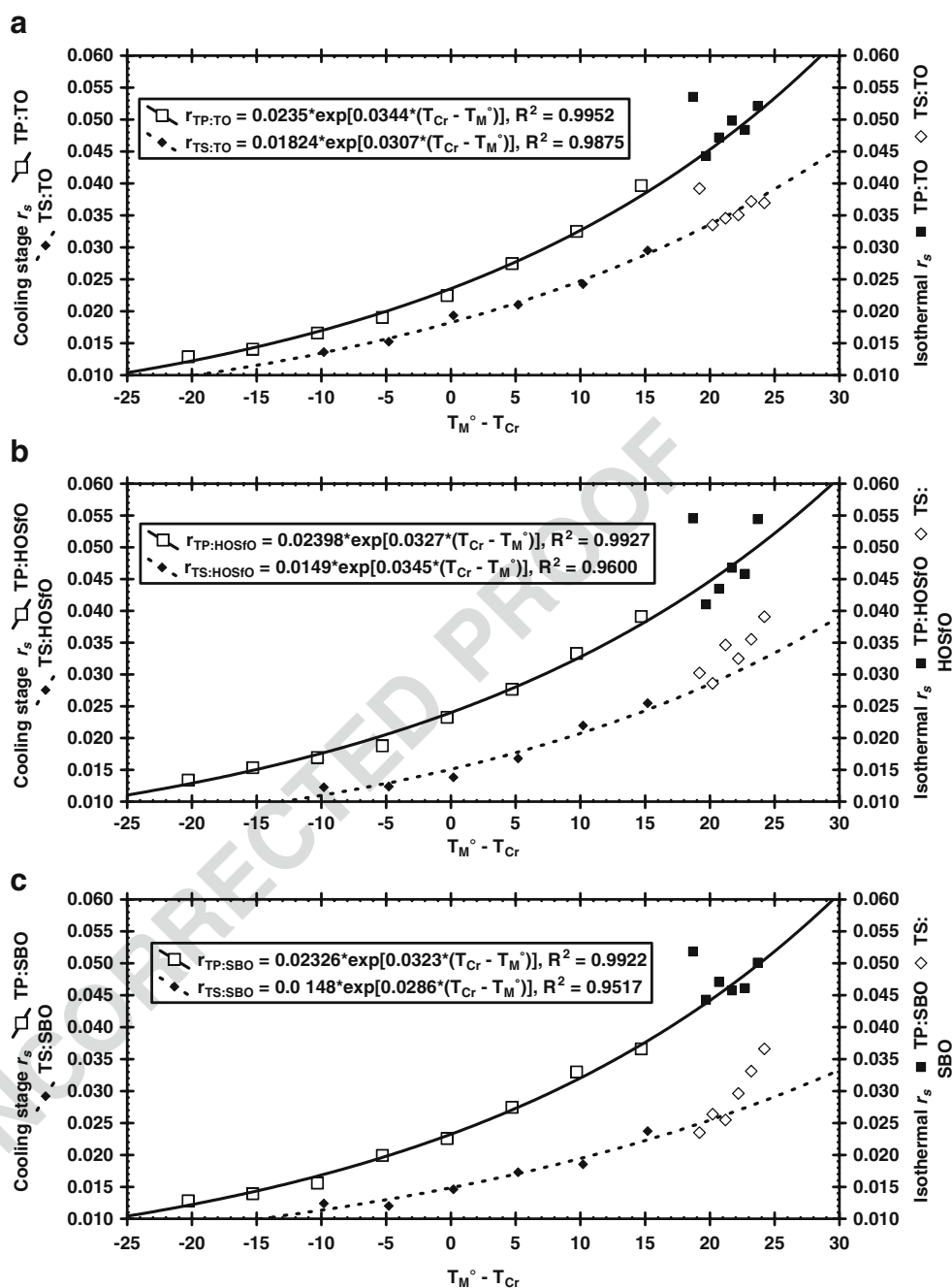
279 During the cooling stage, all blends investigated showed  
 280 an exponential increase of  $r_s$  (i.e., TAGS achieved a higher  
 281 level of liquid structure) as supercooling increased  
 282 ( $R^2 > 0.95$ ; Figure 2). Nevertheless, TP and TS blends  
 283 showed some distinctive features of how  $r_s$  changed as a

function of supercooling. Thus, all TP blends observed  
 similar  $r_s$  values and its change as a function of super-  
 cooling was independent of the type of blend [i.e., the same  
 equation fitted the  $r_s$  vs.  $(T_M^o - T_{Cr})$  data for the three TP  
 blends;  $r_s = 0.0236 \times \exp[0.0331 \times (T_{Cr} - T_M^o)]$ ,  $R^2 = 0.9914$ ].  
 In the same way, TAGS in the liquid state were more  
 structured in the TP blends than in the TS blends (i.e.,  
 overall TS blends showed lower  $r_s$  values than the TP  
 blends). Additionally, in the TS blends the  $r_s$  values showed  
 the following order TO > HOSfO > SBO. However, as  
 observed for  $\Delta G_c$ , the  $r_s$  values for TS/SBO and  
 TS/HOSfO blends were not statistically different.

From the above, we conclude that during the cooling  
 stage, the addition of TP to TO, HOSfO, and SBO did not  
 modify the original TAGS liquid structure. Such behavior  
 was followed for all TP blends at the different  $T_{Cr}$ s used for  
 isothermal crystallization (Figure 2). In contrast, the



**Fig. 2**  $r_s$  as a function of supercooling for the TP and TS blends with TO (a), HOSfO (b), and SBO (c) during the cooling stage and at the  $T_{Cr}$  used for isothermal crystallization. The fitting equations show considered  $r_s$  values just during the cooling stage

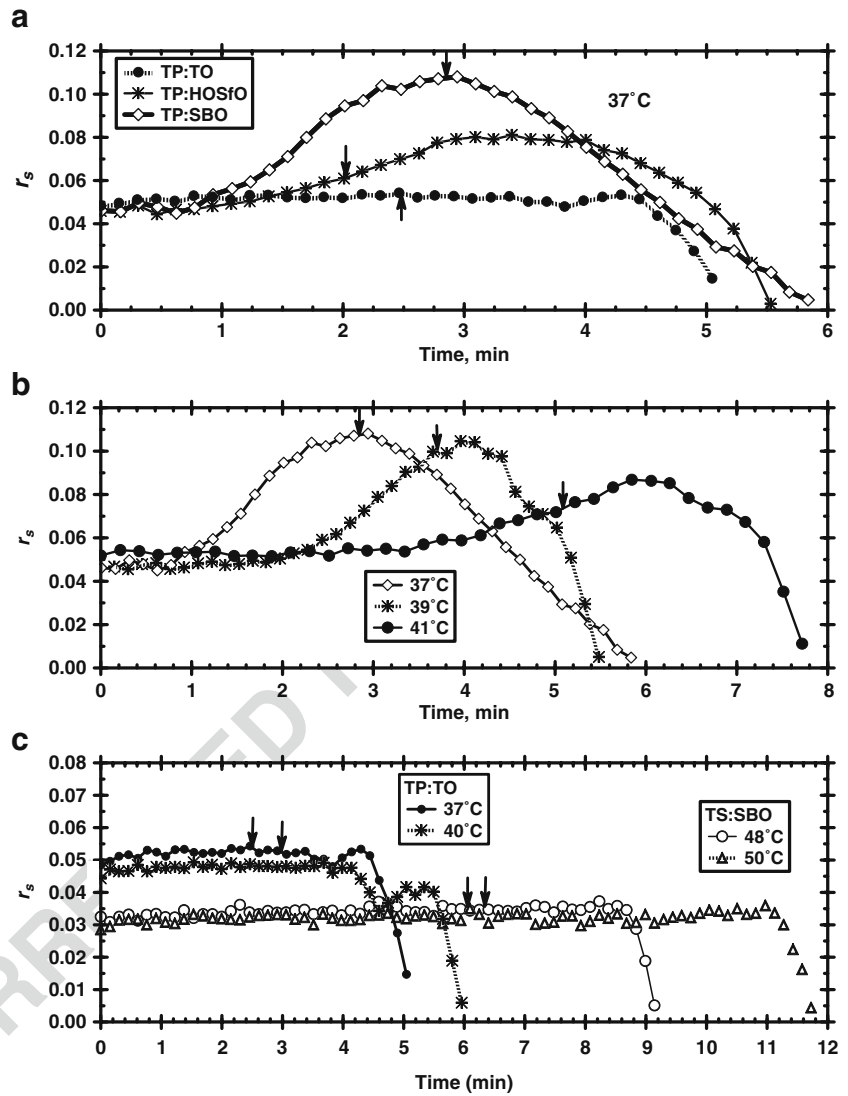


301 addition of TS resulted in decreasing the TAGS liquid  
 302 structure particularly in the TS/HOSfO and TS/SBO blends.  
 303 Additionally, except for the TS/TO blend,  $r_s$  in the  
 304 TS/HOSfO and TS/SBO blends showed a significant  
 305 change in the slope once isothermal conditions were  
 306 achieved (Figure 2). This change in the behavior of  $r_s$  at such  
 307 supercooling conditions (i.e.,  $T_{Cr,s} \leq 51^\circ\text{C}$ ), was associated  
 308 with the developing of a higher TAGS structural organization  
 309 than the one anticipated by the exponential fitting of  $r_s$  during  
 310 the cooling stage (Figure 2). Thus, before  $t_i$  was achieved  
 311 TAGS in the TS/HOSfO and TS/SBO blends accomplished a  
 312 particular structural organization. Since the TS/TO blend did

313 not show this change in the slope (Figure 2), TAGS  
 314 structuring in the liquid state was not associated to triolein.

315 According to the TAGS analysis previously reported<sup>5</sup>,  
 316 HOSfO had about 10% of TAGS containing palmitic acid  
 317 in their composition whereas SBO had approximately 30%  
 318 of these TAGS. Thus, the lower  $r_s$  values observed in the  
 319 TS/HOSfO and TS/SBO blends in comparison with the  
 320 ones observed in the TS/TO blend and the extent of change  
 321 in the slope observed in the TS blends (Figure 2), might be  
 322 associated with the concentration of TAGS containing  
 323 palmitic acid present in the blend. Thus, a more pronounced  
 324 slope change was observed in the TS/SBO blend than in the

**Fig. 3** Evolution of  $r_s$  under isothermal conditions for TP/TO, TP/HOSfO, and TP/SBO blends at a  $T_{Cr}=37^\circ\text{C}$  (a), TP/SBO blends (b), TP/TO and TS/SBO blends (c) at different  $T_{Cr}$ . The arrows indicate the induction time for crystallization ( $t_i$ ) for the corresponding blends



325 TS/HOSfO, and no change was observed in the TS/TO  
 326 blend. The molecular interaction of TS with POO, LLP, and  
 327 PLO/POL seems to occur well before achieving super-  
 328 cooling conditions that resulted in TAGS crystallization  
 329 (i.e., during the cooling stage). TO, HOSfO, and SBO do  
 330 not contain TAGS with stearic acid, and since stearic acid  
 331 has a longer hydrocarbon chain length than palmitic acid,  
 332 structural compatibility between TAGS containing palmitic  
 333 acid and TS was not effective. The result was a decrease in  
 334 TAGS liquid structure and therefore, lowers  $r_s$  values in the  
 335 TS/HOSfO and TS/SBO blends. Once supercooling condi-  
 336 tions required for TAGS crystallization were prevalent (i.e.,  
 337  $T_{Cr} \leq 51^\circ\text{C}$ ), palmitic acid present in the TAGS facilitated  
 338 TS nucleation. As a result,  $\Delta G_c$  was lower in the TS/HOSfO  
 339 and TS/SBO blends compared with the activation energy  
 340 required by TS in the TS/TO blend (Table 2). Probably,  
 341 under such supercooling conditions, TAGS with palmitic  
 342 acid acted as template for TS structuring in the liquid state

and from here the change in the slope of the  $r_s$  vs. ( $T_M^\circ -$   
 $T_{Cr}$ ) relationship in the TS/SBO and TS/HOSfO blends  
 (Figure 2). The result was a lower  $\Delta G_c$  for TS crystallization  
 in SBO and HOSfO, in comparison with the  $\Delta G_c$  observed  
 in the TS/TO blend (Table 2).

Once under isothermal conditions, the  $r_s$  values in all  
 TS blends remained constant as a function of time until  $t_i$   
 was achieved (i.e., no solid phase was present). This  
 behavior was observed at all  $T_{Cr}$ s investigated. Examples  
 of such behavior are presented for the TS/SBO blend at  
 the  $T_{Cr}$  of  $48^\circ\text{C}$  and  $50^\circ\text{C}$  in Figure 3c. The decrease in  $r_s$   
 observed after nucleation (i.e., after  $t_i$ ; Figure 3) was  
 associated to light scattering from the nuclei developed.  
 In some cases (i.e., TS/TO at  $49^\circ\text{C}$  and  $50^\circ\text{C}$  and TP/TO at  
 $39^\circ\text{C}$  and  $40^\circ\text{C}$ ; results not shown), after  $t_i$ , we observed  
 an increase in  $r_s$  before decreasing. In our previous paper<sup>5</sup>,  
 we associate this behavior as a structuring of TAGS due to  
 molecular interaction between TS and TAGS containing

361 palmitic acid. However, since this  $r_s$  peak occurred right  
 362 after nucleation, the behavior might be associated to  
 363 remelting of the solid phase due to the heat generated  
 364 during TAGS crystallization with the subsequent increase  
 365 in  $r_s$ . As crystallization continued and more solid phase  
 366 was present, light scattering produced a decrease in  $r_s$ .

367 In contrast to the TS blends, the TP/SBO and TP/HOSfO  
 368 blends showed an increase in  $r_s$  as a function of time under  
 369 isothermal conditions. The increase in  $r_s$  (i.e., TAGS  
 370 structuring) was a direct function of the concentration of  
 371 TAGS containing at least one chain of palmitic acid, i.e.,  
 372 the increase in  $r_s$  followed the order TP/SBO>TP/HOSfO  
 373 and no increase in the TP/TO blend (Figure 3a). For the  
 374 TP/HOSfO (data not shown) and the TP/SBO (Figure 3b)  
 375 blends, the  $r_s$  onset was an inverse function of super-  
 376 cooling, and the extent of its increment was a direct  
 377 function of supercooling. Thus, the molecular interaction of  
 378 TP with POO, LLP, and PLO/POL were time and  
 379 temperature dependent. Such molecular interactions seem  
 380 to make TP nucleation more difficult in the TP/SBO and  
 381 TP/HOSfO blends than in the TP/TO blend. As a result  
 382  $\Delta G_c$  was higher in TS/SBO and TS/HOSfO blends when  
 383 compared with the  $\Delta G_c$  in the TP/TO blend (Table 2).  
 384 Mihara et al.<sup>19</sup> showed that mixtures of TP and POO  
 385 crystallize more slowly than the pure TAGS. This regardless  
 386 an independent crystallization of TP and POO was  
 387 observed in the mixture (i.e., no mixed crystal formation  
 388 occurred)<sup>19</sup>. Probably, the molecular interactions occurring  
 389 in the liquid phase between TP and TAGS with palmitic  
 390 acid resulted in the development of a mixed TAGS lamellar  
 391 liquid structure. This would delay the nucleation of TP,  
 392 until segregation of TP from the mixed TAGS lamellar  
 393 liquid structure occurred. The result was a higher  $\Delta G_c$  for  
 394 TP nucleation as the concentration of TAGS with palmitic  
 395 acid (i.e., LLP, POO, PLO, and PLO) increased in the  
 396 blends (Table 2).

397  
 398 **Acknowledgments** The investigation was supported by grant  
 399 #25706 from CONACYT. We acknowledge and appreciate the  
 400 fellowship from PROMEP for Elena Dibildox-Alvarado through the  
 401 grant PROMEP/103.5/05/1624. The technical support from Concep-  
 402 cion Maza-Moheno and Elizabeth Garcia-Leos is greatly appreciated.

403 **References**

404 1. D. Pérez-Martínez, C. Alvarez-Salas, M.A. Charo-Alonso, E.  
 405 Dibildox-Alvarado, J.F. Toro-Vazquez, The cooling rate effect on  
 406 the microstructure and rheological properties of blends of cocoa  
 407 butter with vegetable oils. *Food Research International* **40**, 47–62  
 408 (2007). doi:10.1016/j.foodres.2006.07.016  
 409 2. D.J. Cebula, D.J. McClements, M.J.W. Povey, P.R. Smith,  
 410 Neutron diffraction studies of liquid and crystalline trilaurin.  
 411 *Journal of the American Oil Chemists' Society* **69**, 130–136  
 412 (1992). doi:10.1007/BF02540562

3. K. Larsson, Molecular arrangement in glycerides. *Fette, Seifen, Anstrichmittel* **74**, 136 (1972). doi:10.1002/lipi.19720740302 413  
 4. R.W. Corkery, D. Rousseau, P. Smith, D.A. Pink, C.B. Hanna, A case for discotic liquid crystals in molten triglycerides. *Langmuir* **23**, 7241–7246 (2007). PMID: 17511482 414  
 5. Dibildox-Alvarado, E., Laredo, T., Toro-Vazquez, J. F., Marangoni, A. G. Pre-nucleation structuring of TAG melts revealed by fluorescence polarization spectroscopy and molecular mechanics simulations, *Journal of the American Oil Chemists' Society* (in press). (2010) 415  
 6. J.F. Toro-Vazquez, E. Dibildox-Alvarado, M.A. Charó-Alonso, V. Herrera-Coronado, C.A. Gómez-Aldapa, The Avrami index and the fractal dimension in vegetable oil crystallization. *Journal of the American Oil Chemists' Society* **79**, 855–866 (2002). doi:10.1007/s11746-002-0570-y 416  
 7. J.D. Hoffman, J.J. Weeks, Melting process and the equilibrium melting temperature of polychlorotrifluoroethylene. *Journal of Research of the National Bureau of Standards* **66**, 13–28 (1962) 417  
 8. D. Pérez-Martínez, C. Alvarez-Salas, J. Morales-Rueda, J.F. Toro-Vazquez, M. Charó-Alonso, E. Dibildox-Alvarado, The effect of supercooling on crystallization of cocoa butter-vegetable oil blends. *Journal of the American Oil Chemists' Society* **82**, 471–479 (2005). doi:10.1007/s11746-005-1096-z 418  
 9. J.F. Toro-Vazquez, M. Briceño-Montelongo, E. Dibildox-Alvarado, M.A. Charó-Alonso, J. Reyes-Hernández, Crystallization kinetics of palm stearin in blends with sesame seed oil. *Journal of the American Oil Chemists' Society* **77**, 297–310 (2000). doi:10.1007/s11746-000-0049-x 419  
 10. W.L. Ng, A Study of the kinetics of nucleation in a palm oil melt. *Journal of the American Oil Chemists' Society* **67**, 879–882 (1990). doi:10.1007/BF02540510 420  
 11. J.W. Litwinenko, A.M. Rojas, L.N. Gerschenson, A.G. Marangoni, Relationship between crystallization behavior, microstructure, and mechanical properties in a palm oil-based shortening. *Journal of the American Oil Chemists' Society* **79**, 647–654 (2002). doi:10.1007/s11746-002-0538-y 421  
 12. C.W. Chen, O.M. Lai, H.M. Ghazali, C.L. Chong, Isothermal crystallization kinetics of refined palm oil. *Journal of the American Oil Chemists' Society* **79**, 403–410 (2002). doi:10.1007/s11746-002-0496-4 422  
 13. M. Cerdeira, V. Pastore, L. Vera, S. Martini, R.J. Candal, M.L. Herrera, Nucleation behavior of blended high-melting fractions of milk fat as affected by emulsifiers. *European Journal of Lipid Science and Technology* **107**, 877–885 (2005). doi:10.1002/ejlt.200500257 423  
 14. A. Minato, S. Ueno, K. Smith, Y. Amemiya, K. Sato, Thermodynamic and kinetic study on phase behavior of binary mixtures of POP and PPO forming molecular compound systems. *The Journal of Physical Chemistry. B* **101**, 3498–3505 (1997). doi:10.1021/jp962956v 424  
 15. S. Ueno, A. Minato, J. Yano, K. Sato, Synchrotron radiation X-ray diffraction study of polymorphic crystallization of SOS from liquid phase. *Journal of Crystal Growth* **198**, 1326–1329 (1999). doi:10.1016/S0022-0248(98)01018-5 425  
 16. K. Larsson, On the structure of the liquid state of triglycerides. *Journal of the American Oil Chemists' Society* **69**, 835–836 (1992). doi:10.1007/BF02635928 426  
 17. L. Hernqvist, On the structure of triglycerides in the liquid state and fat crystallization. *Fette Seifen Anstrichmittel* **86**, 297 (1984) 427  
 18. J.F. Toro-Vazquez, A. Gallegos-Infante, Viscosity and its relationship to crystallization in a binary system of saturated triacylglycerides and sesame seed oil. *Journal of the American Oil Chemists' Society* **73**, 1237–1246 (1996). doi:10.1007/BF02525452 428  
 19. H. Mihara, T. Ishiguro, H. Fukano, S. Taniuchi, K. Ogino, Effect of crystallization temperature of palm oil on its crystallization. IV. The influence of tripalmitoylglycerol (PPP) on the crystallization of 1, 3-dipalmitoyl-2-oleoyl-glycerol (POP) and 1, 2, dioleoyl -3-palmitoyl-glycerol (POO). *Journal of Oleo Science* **56**, 223–230 (2007). PMID: 17898485 429  
 430  
 431  
 432  
 433  
 434  
 435  
 436  
 437  
 438  
 439  
 440  
 441  
 442  
 443  
 444  
 445  
 446  
 447  
 448  
 449  
 450  
 451  
 452  
 453  
 454  
 455  
 456  
 457  
 458  
 459  
 460  
 461  
 462  
 463  
 464  
 465  
 466  
 467  
 468  
 469  
 470  
 471  
 472  
 473  
 474  
 475  
 476  
 477  
 478

## **IV. CONCLUSIONES GENERALES**

## **CONCLUSIONES GENERALES**

En conclusión, este trabajo estudió el ordenamiento previo a la nucleación que ocurre en mezclas de TAGS saturados con diferentes aceites vegetales líquidos. Los experimentos por espectroscopia de fluorescencia polarizada dieron una visión sobre la estructuración a nivel microscópico que ocurre en esta etapa. Para aclarar el tipo de interacciones responsables de este efecto a nivel molecular, la simulación MM resultó ser una herramienta rápida y simple para abordar este aspecto y puede proporcionar información complementaria a los datos experimentales, haciendo notar que los resultados obtenidos necesitan ser cuidadosamente interpretados según las condiciones usadas en las simulaciones.

Los resultados obtenidos en esta investigación demostraron que:

- La anisotropía y la viscosidad varían linealmente, de aquí que la anisotropía, en el rango estudiado, es una medida de la microviscosidad del sistema.
- Es posible evaluar por medio de la anisotropía los cambios en la microviscosidad de la fase líquida como efecto de interacciones moleculares que conducen a la estructuración de la mezcla previa a la nucleación y crecimiento de los cristales en sistemas complejos.
- Son las fuerzas van der Waals las responsables del comportamiento líquido o sólido de los TAGS y por lo tanto, piezas clave causantes del aumento en la microviscosidad de un sistema de TAGS previo a su nucleación.
- Ocurre un comportamiento específico en función de la composición molecular de un TAG en particular. Así, la presencia de moléculas que contienen al menos una cadena de

ácido palmítico en su composición de TAGS, induce a un aumento en la microviscosidad de la mezclas previo a la nucleación y es por lo tanto requisito para inducir una interacción molecular.

- La  $\Delta G_c$  requerida para formar núcleos estables de un TAG saturado (ej., TP) es mayor a medida que la concentración de TAGS con ácido palmítico (ej., LLP, POO y PLO/POL) aumenta en las mezclas.

Aunado a lo anterior, en general se logró una mejor comprensión de las interacciones moleculares responsables de un fenómeno observado experimentalmente. Además, es nuestra expectativa el que este trabajo haya establecido las bases para la aplicación de simulaciones MM en sistemas similares a los aquí presentados.